**TECHNISCHE
UNIVERSITÄT
WIEN**

**VIENNA
UNIVERSITY OF
TECHNOLOGY**

D I S S E R T A T I O N

Multiscale Blood Flow Modelling and Simulation

ausgeführt zum Zwecke der Erlangung des akademischen Grades eines
Doktors der technischen Wissenschaften unter der Leitung von

ao.Univ.-Prof. Dipl.-Ing. Dr.techn. Felix Breitenecker

eingereicht an der Technischen Universität Wien
bei der Fakultät für Mathematik und Geoinformation

von

Dipl.-Ing. Johannes Kropf

Matrikelnummer: 9630213
Brachelligasse 28/7
1220 Wien

Wien, im September 2007

Acknowledgement

Abstract

Due the more and more sophisticated medical care in western countries the main causes of death is moving against diseases of the cardiovascular system like heart attacks, arteriosclerosis or apoplectic strokes. Hence it is not surprising that a lot of researchers are going to the time and effort of researching on that field. Especially the arterial part of the cardiovascular system is of fundamental interest because of its transport features.

Modelling and simulation of the cardiovascular system have a long tradition, but mainly during the last century a big amount of models for the simulation of blood flow and pulse wave propagation in arteries were developed. Since the first compartment model published in 1733 by Stephen Hales [13] a huge amount of different models emerged. From very simply lumped parameter models without consideration of control mechanism to very complex 3-dimensional models for the blood flow in systemic arteries the reader can find a lot of scientific works in literature. All this models have its advantages as well as its disadvantages, depending on the aim of the simulation. The simple models may not map the physiological properties properly and the complex models are too hard to handle or they consider only a small part of the whole cardiovascular circle.

This work tries to find the happy medium and a dynamic controlled and identifiable multiscale model for the whole cardiovascular cycle is developed. The validity of the model is verified by measured data. Doing this, several different types of models are discussed and chosen to be connected to the final overall model.

In detail this work covers the implementation of an one-dimensional dynamic

model for the big systemic arteries based on the incompressible Navier-Stokes equations and its connection with a lumped parameter model of six compartments. Additionally, a model for the small arteries is used for determination of boundary values for the termination segments of the modelled vascular bed. Within the compartment model two physiological control mechanisms are considered. To connect the models to each other they have to be synced at first since they operate on different time scales. While the solution of the controlled compartment model is straight forward by quadrature, solving the dynamic Navier-Stokes model is more sophisticated. Here we used a finite volume method implemented by Wibmer [55].

A fundamental part of this work deals with the identification of the coupled dynamic multiscale model based on measured data. To do this, several so-called *alternative models* are tested to be able to compute as much as possible unknown parameters from an usually quite fragmentary set of measured data. Basically, two classes of parameters have to be computed. On the one hand the geometrical and physical structure of the vascular bed, mainly of the big systemic arteries has to be determined (i.e. vessel diameters, lengths and elasticity), on the other hand by reason of the used computational methods terminal conditions have to be fulfilled. For instance, we use Windkessel models on termination segments of the arterial tree whose parameters have to be known.

From ultrasound measurement we are able to achieve physical data of the vascular bed of several positions. By help of other datasets from literature the missing data are extrapolated. Due the usage of an additional electro-cardiogram (ECG) the pulse wave velocity can be measured as well what is used for determining the vessel wall elasticity.

The Windkessel data are computed through a linearised model for the cardio-vascular tree each time step in the scale of the compartment model. Doing this, a model for the small arteries based on the linearised Navier-Stokes equations is used.

All this was implemented in JAVA and C++ and a simulation and identification tool for the human arterial system emerged.

Kurzfassung

Heute verlagert sich die Haupttodesursache aufgrund der immer besser werdenden medizinischen Versorgung und dem dadurch immer höher werdenden Alter der Menschen in der westlichen Welt immer mehr auf Erkrankungen des kardiovaskulären System. Herzversagen und Arteriosklerose sind nur einige der Ursachen. So wundert es nicht weiter das sich viele Forschungen im medizinisch-technischen Bereich auf das arterielle Kreislaufsystem konzentrieren, welches aufgrund der Transporteigenschaften von zentraler Bedeutung ist. Auch in dieser Arbeit wird vor allem auf die Modellierung des arteriellen Teils eingegangen.

Simulation des arteriellen Blutkreislaufs hat eine lange Tradition. Während des letzten Jahrhunderts wurden eine Vielzahl von Modellen zur Simulation des Blutflusses und der Pulswellenausbreitung in den Gefäßen entwickelt. Seit dem ersten Kompartment Modell von Stephen Hales aus dem Jahr 1733 [13] entstanden die verschiedensten Modelle, die Teile des arteriellen Systemkreislaufs abbildeten, bis hin zu globalen Modellen für den gesamten Blutkreislauf und 3-dimensionalen Strömungsmodellen der Arterien. So verschieden die Modelle sind, so sind es auch ihre Lösungsmethoden. All diese verschiedenen Ansätze haben ihre Vor- und Nachteile, abhänging vom verfolgten Ziel der Simulation. Die einfachsten Modelle haben zu wenig Aussagekraft da sie zu wenige physiologische Phänomene abbilden, zu komplexe Modelle sind aufgrund der großen Anzahl an unbekannten Parametern nicht identifizierbar.

Diese Arbeit versucht einen optimalen Mittelweg zu finden um ein globales dynamisches geregeltes und identifizierbares Modell für den menschlichen

Herzkreislauf zu entwickeln und die Gültigkeit des Modells anhand von Mess-
daten zu verifizieren. Um das zu bewerkstelligen wurden verschiedene Model-
lansätze gewählt und miteinander gekoppelt.

Im Speziellen wird in dieser Arbeit ein 1-dimensionales Strömungsmod-
ell auf Basis der inkompressiblen Navier-Stokes Gleichungen mit einem 6-
Kompartmentmodell für den Regelkreislauf verknüpft. Die beiden Modelle
arbeiten auf verschiedenen Zeitskalen die synchronisiert werden müssen.

Während das Kompartmentmodell mittels einfacher Quadratur gelöst wer-
den kann, sind zur Lösung der partiellen Navier-Stokes Differentialgleichun-
gen komplexere Methoden erforderlich. Hierzu wurde auf die Lösung von
Wibmer [55] mit einem finite Volumen Verfahren zurückgegriffen. Andere
Methode wie zum Beispiel finite Elementen oder finite Differenzen finden
sich z.B. in [8, 12, 38].

Der Hauptteil der Arbeit beschäftigt sich mit der Identifizierung des gekop-
pelten multiskalen Modells auf Grund von Messdaten. Dazu wurden eine
Reihe von so genannten *Ersatzmodellen* untersucht um von der beschränk-
ten Anzahl an verfügbaren Daten auf die fehlenden Daten rückzurechnen.
Prinzipiell sind aus den Messdaten zweierlei Parameter zu bestimmen; zum
einen muss die Struktur des Arteriennetzwerks (d.h. Arteriendurchmesser,
Längen, Elastizität) angepasst werden, zum anderen die Parameter der
Randbedingungen die durch die verwendeten Methoden auftreten, bestimmt
werden. Viele dieser Parameter sind nicht direkt messbar und müssen indi-
rekt durch andere Modelle bestimmt werden. Da die Randbedingungen von
den zu berechnenden Größen abhängen, müssen diese in jedem Zeitschritt
neu bestimmt werden wofür einfach zu berechnende Ersatzmodelle notwendig
sind. Im Speziellen werden so Elasitizität und Windkesseldaten an den End-
segmenten des modellierten Arteriennetzwerkes berechnet.

Im Rahmen der Dissertation konnte auch eine Studie mit freiwilligen Proban-
den durchgeführt werden in der kardiovaskuläre Parameter erhoben wurden.
Diese Daten dienen dann am Ende dieser Arbeit zum einen als Grundlage der
Identifizierung des dynamischen geregelten Kreislaufmodell und zum anderen
zur Verifizierung der errechneten Daten wie Pulsdruckkurven oder Flusskur-
ven.

Contents

Chapter 1

Introduction

"A theory is something nobody believes, except the person who made it. An experiment is something everybody believes, except the person who made it."

Albert Einstein

Nowadays the largest amount of deaths in industrial countries can be ascribed to diseases of the cardiovascular system, like atherosclerosis, hypertension or cardiac insufficiency. Therefore it not surprising that research on this field is of big interest and a lot of investigators are trying to explain the systems complex physiological behaviour, which is still not fully understood. A huge amount of different physiological functions are influencing each other in a very complex way.

From today's technical point of view non-invasive measurement techniques for the determination of physiological parameters are of high interest and a wide diversity of devices is available and under development. Especially the measurement of cardiovascular parameters like pulsatile blood pressure, cardiac output, blood volume flow and peripheral resistance are of essential

importance in modern medical diagnostics. Mathematical models can provide a powerful tool for interpretation and indirect measurement of further properties.

Also in the field of modelling and simulation of the cardiovascular system (CVS) a lot of work was done during the last hundred years. The great advantage of investigating mathematical models instead of living individuals or animals is obvious, even it cannot be a complete replacement for research on living mammals. Mathematical models based on physical laws can explain a lot of effects observed. Starting with models for mathematical description of pulse wave propagation and simple models for the aortic Windkessel effects at the beginning of the 20th century, today very complex models in three dimensions for modelling turbulent flow in bifurcations are available. Also the fast development of computers during the last two decades was very helpful for research and the development of highly sophisticated mathematical models which are solved numerically.

Although research on blood flow in arteries started long time ago only a few researchers worked on this topic until the 1950s since a huge amount of investigators started to develop models by using different kind of approaches. When simulating blood flow and pressure waves in arteries the governing equations for an incompressible fluid in an elastic or viscoelastic domain have to be solved. Doing this at least four approaches are possible. The first approach is the use of lumped parameter models. These models are easy to handle, cheap in computing time and have less parameters to identify. Usually these models are compartmental based and cover the whole human cardiovascular system including the pulmonary and venous part in contrary to the other approaches. But transient behaviour of the pressure and flow waveforms can not be studied.

The second approach, the one-dimensional wave propagation method, involves solving the governing equations of blood flow in a one-dimensional domain and is based on the assumptions that the dominant component of blood flow velocity is oriented along the vessel axis and that the pressure can be assumed to be constant over the cross-section of the vessel [50]. Assuming

further a Newtonian fluid in a deforming, impermeable, elastic domain, these nonlinear partial differential equations consist of the continuity equation, a single axial momentum balance equation and a constitutive equation. Additionally boundary conditions have to be drawn up. A lot of solutions of this approach can be find in the literature solved by different numerical methods like finite difference schemes, finite elements or finite volume methods [38, 41, 50, 53, 55].

A third approach is based on the Womersley solution for pulsatile flow in elastic vessel [56, 57, 58]. Here, some more assumptions were made, namely asymmetry, linear constitutive behavior and small perturbations about a constant pressure and zero axial velocity reference state. Then, a system of linear partial differential equations can be derived and solved analytically. A solving strategy can be to prescribe flow and impedance at the aortic root and determine characteristic impedances for the arterial segments like Avolio did in [3]. While these impedance-based linear models can be used to prescribe flow and pressure at the aortic root, they do not incorporate nonlinear advective losses or losses due to branching and stenoses [32, 46, 50, 51]. Especially applied to blood flow in the major arteries this is perhaps the most significant limitation of Womersley's theory.

The forth approach to model blood flow and pressure wave forms in human arteries is to solve the three-dimensional Navier-Stokes equations numerically in elastic domains. It requires also appropriate boundary conditions. While the prescribed velocity, volume flow or pressure, depending on the formulation, can be computed, the quantities for the blood flow exiting the vessels in the terminal segment of the branch is unknown and part of the desired solution [5, 7, 20, 35].

Due to the goal of this work is to gain an identifiable and controlled dynamic model for simulating blood flow and pressure wave forms in the major arteries we make use of the first three of the approaches mentioned above. For getting pressure and flow wave forms in systemic arteries it is not necessary to compute them also in the venous part, but because of the systems' control it can not be neglected and therefor parts of minor interest are governed by

simpler lumped parameter models, so that only very less physical parameters have to be identified. The parts of interest within the vascular system are modelled in a more detailed way. All of them are combined to a big model which let us consider the behaviour of the whole system.

Within this work the focus is on models for termination segments of the vascular bed and its coupling with models for control and blood flow in arteries. During investigation it became obvious that this is a quite difficult task. Additionally its parameters cannot be identified directly by measurement and so other indirect methods became necessary.

For the combination of models of different scales a good understanding of the physiological coherences is necessary what should be given with this work also. Starting with some haemodynamical fundamentals given in the next section, an introduction into mathematical modelling of fluid dynamics is covered by the second chapter.

The most common-sense strategy in modelling complex systems is the bottom-up approach. The three basic concepts of cardiovascular modelling, on which all other models developed later are based on, are explained in the third chapter. Using the bottom-up principle, the compartmental model with control mechanisms covering the whole CVS is given in the following chapter. After that a more detailed linearised model for the systemic arteries, which is the part of interest in investigation of cardiovascular diseases, is developed in chapter five.

The third and last approach considered within this thesis is a non-linear approach solving the Navier-Stokes equations for elastic tubes. This numerically solved model handles a huge amount of effects observed in natural environment, but identifying its parameters is a difficult task for which the other more simple models are used.

The aim of this work is to develop a controlled and identifiable model of the whole CVS and therefore the different models mentioned above are connected to each other, what is the content of the seventh chapter. In the last chapters an overview of the implementation of the whole model with all its approaches is given and the results of simulation runs are presented. For

better readability some complex formulas and tables of measured data are sourced out to the appendix and its sections are referred in the context.

1.1 Modelling and Simulation

For a huge amount of problems in applications quantitative as well as qualitative propositions are claimed to be emerged from the solution. Only in some very simple cases both can be done directly. Usually the use of mathematical methods is necessary, even a lot of obviously empiric solutions are based on an abstract model behind. Nowadays we are able to use more and more complex systems of a better understanding of natural processes (e.g. healing of diseases). The basic tools for it are mostly mathematical models, i.e. formal descriptions using mathematical formalism like equations or graphs.

Simulation is a method beyond a lot of others to solve problems in different applications. The concept of simulation might be described well by

"Simulation is the replication of a dynamic process in a model to get insights which are transmittable to the real world"

Modelling and simulation is an iterative process where the model has to be adapted to the real world recurrently. Hereby the incessant interaction of the different steps is essential. Observations lead to a model and the results of the simulation at their part lead to observations again, on which the validation of the model is based.

1.1.1 Types of Models

A model is the description of a concrete system. Dependent on the based approach different kinds of models are distinguished. A classification of models discussed within this work is given in the following section.
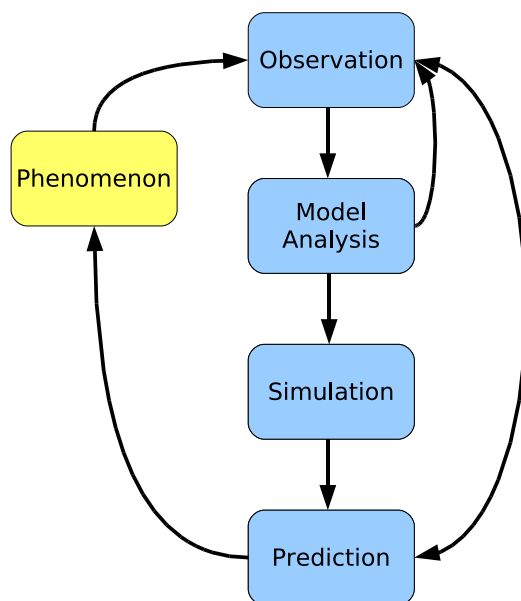
Figure 1.1: *Scheme of a simulation study*

Structural Models

The geometrical structure of the arterial tree is mapped onto the model where the physical parameters and physiological properties are considered. This is the most detailed variant we are using, but it leads also to a higher complexity and computational efforts.

Lumped Parameter Models

By using this kind of models the geometrical structure of the aterial tree is not mapped, but the behaviour of the cardiovascular properties and its regulation process is considered in a global way. To do this the arterial tree is *lumped* to so called compartments which are investigated with our model. It is clear that there are huge restrictions on using such kind of models, but they are much more simpler and the amount of unknown parameters is smaller. For instance with a lumped parameter model also the solution is lumped, for example the blood pressure is gained only as a mean value, not as a transient wave form.

Alternative Models

Sometimes the underlying physical procedures are not known or are too complex for modelling it in a practical way. In this case it can be a good choice to use *alternative models*. Instead of mapping the structure of the cardiovascular bed, the behaviour of the considered process is the basis of the model. The most prominent example for this type of models is the so called *Windkessel* model on which we will refer often within this work. Parts of the arterial tree *behave* like a Windkessel and so we can use it as a simplified alternative model.

Models for Boundary Data

Due to the complexity of the human physiology only parts of the internal procedures can be considered. Under such restrictions it follows that one has to deal with unknown boundary parameters indispensably. For modelling this artificial splitting the use of alternative models is necessary. This way are modeled parts of the system which are not considered by the simulation, but which are necessary to close the circle. In our special case the boundary data at the entry respectively the exit of the system, namely the vessel tree of the large arteries. We need a model for the heart, with it the blood flow is driven, as well as a model for the small arteries which are not concerned by our approach by default. The small arteries cannot be modeled like the large ones cause of the lack of measured data and the very wide branched structure which is not known. We just know how they behave and try to simulate its phenomenons. Also the elasticity of the vessel walls is mapped by such an alternative model, based on observations. All this models are dynamic, that means time dependent, contrary to the model parameters, which are constant, and model variables which are determined by the model itself.

1.2   Haemodynamical Basics

The overall arrangement of the human cardiovascular system can be summarised briefly as follows (compare [34]).

The system is driven by the heart, which is composed of four chambers, arranged in two pairs. Two of the chambers, the atriums are thin-walled, and connected through valves to the thick-walled ventricles, one on each side. From there, blood is pumped into the aorta (left ventricle) and into the lungs (right ventricle). The left ventricle is more muscular then the right one to produce enough pressure to pump oxygenated blood through the body. Furthermore, the left ventricle is connected to the aorta, the main and largest artery in the human body with a diameter of approximately 2.5 cm. Large arteries branch of the aorta and the arteries became smaller and smaller until they reach a diameter of 30-100 μm in the arterioles. These small arteries end in the capillaries with a diameter down to 4 or 5 μm. These very fine vessels converge again in the venous system which has other mechanical properties as the arterial part. In this work only the arterial system will be considered.

The walls of bloodvessels have a similar structure in the whole body. They are made up of similar materials, although their proportions vary in different parts of the system. Traditionally the wall is divided into three layers, the innermost intima, the media and the outermost adventitia. The inner intima consists of two parts, the endothelium, which is a single layer of cells, and surrounding it, a thin subendothelial layer containing collagen fibres. The most important part of the vesselwall when considering mechanical properties is the media. The inner boundary is formed mainly by a layer of interlinked elastin fibres, called the internal elastic lamina. The rest of the media, which is usually the thickest part of the vessel wall, differs in the structure from large to small arteries. In larger arteries it consists of multiple concentric layers of elastic tissue (elastin), separated by thin layers of connective tissue, called collagen and smooth muscle cells. In smaller arteries the media consists mainly of this smooth muscle cells with thin layers of elastin and collagen in between. After another thin elastic layer the adventitia is connected outside. Although it is as thick as the media it plays an unimportant

rule for mechanical properties, it consists of very loose tissue.

The vessels consist of elastin, collagen and smooth muscle fibres of about 50%, the rest is water which has a negligible effect on the mechanical properties. The difference of elasticity of arteries from the proximal to the distal end is caused by the ratio of elastin to collagen. In the intrathoracic aorta the ratio is about 1.5, while in other arteries, which are more stiffer, the ratio decreases to about 0.5.

It is clear that the mechanical properties of the vessel walls depend on both on the properties of its individual components and on how they are connected together. Elastin is a very elastic material and can be extend easily. Collagen is much stiffer with a Young's modulus of about $10^6 kNm^-2$. Smooth muscle has a Young's modulus similar to that of elastin, but its actual value depends on the level of physiological activity, varying from $100kNm^{-2}$ in the relaxed state to $1200kNm^{-2}$ in the active state. But only elastin is purely elastic, the others, especially smooth muscles show viscoelastic properties what is reflected in dynamic properties of artery walls.

1.2.1   Viscoelasticity of the Blood Vessels

In basic considerations of the pressure-flow relationships of oscillatory flow the artery is treated as a cylindrical tube of constant diameter. In reality, an artery is a viscoelastic tube whose diameter varies with a pulsatile pressure and whose elasticity varies therefore with time and frequency. The mechanical properties of the vessel wall are well investigated and its results can be found in literature [4, 31, 34, 36].

To study haemodynamics of the arterial system knowledge of the elastic properties of the arterial wall is of fundamental importance. Indeed, knowledge of the viscoelastic properties of the blood vessels has long been recognized as playing an essential role in cardiovascular behaviour.

Relations between forces applied to a body and its deformation is covered by the theory of elasticity. The force per unit area producing the deformation is called the *stress* whereby the ratio of the deformation to its original form is called *strain*. Because its a ratio, *strain* is dimensionless. Although the

ability to withstand a stress is a property that distinguishes a solid from a liquid, a larger number of substances exhibit properties appropriate to an elastic solid as well as a viscous liquid. Blood vessels belong to this huge class of so called *viscoelastic* materials. The deformation of such materials depends on both the magnitude of the stress and the rate at which is applied.

Of course no substance is perfectly elastic when very large forces are applied to it, but for small deformations it is proportional to the force and linear. This proportionality was first described by Robert Hooke (1635-1703) in 1676 and is well known as Hooke's law. With larger forces this proportionality ceases and this limit is known as *elastic limit*. The material cannot regain to its original form beyond this point. With further increasing of the load the *yield point* will be reached and usually leads to breakage.

The classical theory of elasticity is based on two fundamental assumptions, namely the substance is continuous and uniform or homogeneous but neither of the two applies well to the arterial wall. At first, the wall is highly extensible and behaves more as rubber, and at second, the main elastic components as mentioned in the latter section, are collagen and elastin which a fibrous and supported in a liquid of water and mucoproteins. Therefore the arterial wall is far from being homogeneous. Nevertheless the main analyses of the arterial mechanics are based on classical theory.

Strain and Stress

Referring to its consequence strain is divided in *longitudinal* strain when a body is extended from a length x_0 to a length x_1, to *compressive* strain when there is a change of volume and to *shear* strain when there is an displacement of two points in parallel planes in a direction parallel to those planes.

The *longitudinal* stress is expressed by

$$\epsilon_{xx} = \frac{x_1 - x_0}{x_0} \tag{1.1}$$

while in the y or z direction the strains are given by

$$\epsilon_{yy} = \frac{y1 - y_0}{y_0} = -\sigma_{yx}\epsilon_{xx} \tag{1.2}$$

and

$$\epsilon_{zz} = \frac{z_1 - z_0}{z_0} = -\sigma_{zx}\epsilon_{xx} \tag{1.3}$$

where σ, the ratio of transverse to longitudinal strain, is called *Poisson ratio*. σ is a characteristic property of the material and for small strain its constant, but it cannot necessarily be assumed that $\sigma_{yz} = \sigma_{zx}$. That holds for so-called *isotropic* materials where the elasticity is the same in all directions. Practically, for the Poisson ratio the effective range is $0.0 - 0.5$. For small extensions with a ratio 0.5, the volume of a solid remains constant when it is stretched.

In three dimensions we get one tensile and two shearing strains for every plane. After taking into account that ϵ_{xy} and ϵ_{yx} are identical we gain six independent components

$$\epsilon_{xx}, \epsilon_{xy}, \epsilon_{yy}, \epsilon_{yz}, \epsilon_{zz}, \epsilon_{zx}.$$

and six corresponding Poisson ratios

$$\sigma_{xx}, \sigma_{xy}, \sigma_{yy}, \sigma_{yz}, \sigma_{zz}, \sigma_{zx}.$$

Strain is caused by a force F acting across a given plane in a body. Thus the unit of this force F is $\frac{F}{A}$, called *stress*.

The stress on a point in a plane may be resolved into those normal (tensile stress) and tangential (shear stress). The components along the three axis are designated by subscripts where the capital letters indicate the direction of

a stress component. Because X_y and Y_x must be equal to prevent rotational resultant we therefore left with six independent components of stress:

$$X_x, \ X_y, \ X_z, \ Y_x, \ Y_z, \ Z_z, \ Z_x$$

The Relationship between strain and stress

The relationship between stress and strain is expressed as an elastic modulus. As strain is dimensionless, all these moduli will have the dimension of stress (i.e. force per unit area).

The modulus in longitudinal direction (stress and strain are considered in the same direction) is called *Young's modulus* in honor of the pioneer work of Thomas Young (1808) and is designated by E.

$$E = \frac{X_x}{\epsilon_{xx}} \tag{1.4}$$

In this work the Young's modulus will refer to the Young's modulus in circumferential direction further on. Other definitions of elastic modulus like *shear modulus* or *bulk modulus* are not used here and therefore not discussed. For further details the reader may refer to [31] and references therein.

As the dynamic behavior of the arterial wall is the periodic strain imposed by the pulse wave the response of the wall to a stress is often analysed by a stress of a harmonic function. In this case, the viscous elements will cause a phase lag of angle ϕ between stress and its resultant strain.

McDonald [31] mentioned the first formulation by Hardung [14, 15, 16] who introduced the elastic modulus E' in complex form:

$$E' = E_{dyn} + i\mu\omega \tag{1.5}$$

where the real part E_{dyn} is given by

$$E_{dyn} = \frac{\Delta P}{\Delta l} \frac{l_m}{q_m} \cos\phi \tag{1.6}$$

and the imaginary part by

$$\mu\omega = \frac{\Delta P}{\Delta l}\frac{l_m}{q_m}\sin\phi; \qquad (1.7)$$

l_m and q_m are the average length and the cross-section of the specimen. In the upper formulas μ denotes the dynamic viscosity and ω the concerned frequency.

Although the dynamic elastic modulus is rising continuously with frequency, in arterial wall it increases markedly up to a frequency below 2 Hz and thereafter remains constant.

1.2.2 Wave form analysis

The arterial pulse has been recognized from antiquity as the most fundamental sign of life. A huge number of scientific publications dealing with that topic can be found. Marey [42] was the first who obtained accurate results recording arterial pressure pulses with non-invasive measuring methods where invasive methods were used before like Frank [9, 10] did with his manometer for registering intra-arterial blood pressure.

When observing waveforms of flow and pressure in the ascending aorta one can see differences between the shapes of them. As long as cardiovascular physiologists have been able to measure pressure and flow in the ascending aorta, they have puzzled over this phenomenon.

One explanation of this differences could be the existence of wave reflections caused by the peripheral arteries. A reflected back travelling wave that reinforces the pressure will have a cancelling effect on the flow shape. However, it could not be demonstrated yet that wave reflection are sufficient to explain such large, qualitative differences in the aortic pressure and flow waveforms [52]. Milnor [27] remarked that the aortic tree in a young normal animal is a perfect diffuser, i.e, it generates far fewer reflections than any man-made distributed network. Wang et. al. [52] explained these phenomenons with help of simple Windkessel models and verified their assumptions with measurements on dogs. Even with artificial pressure waves generated in the abdomi-
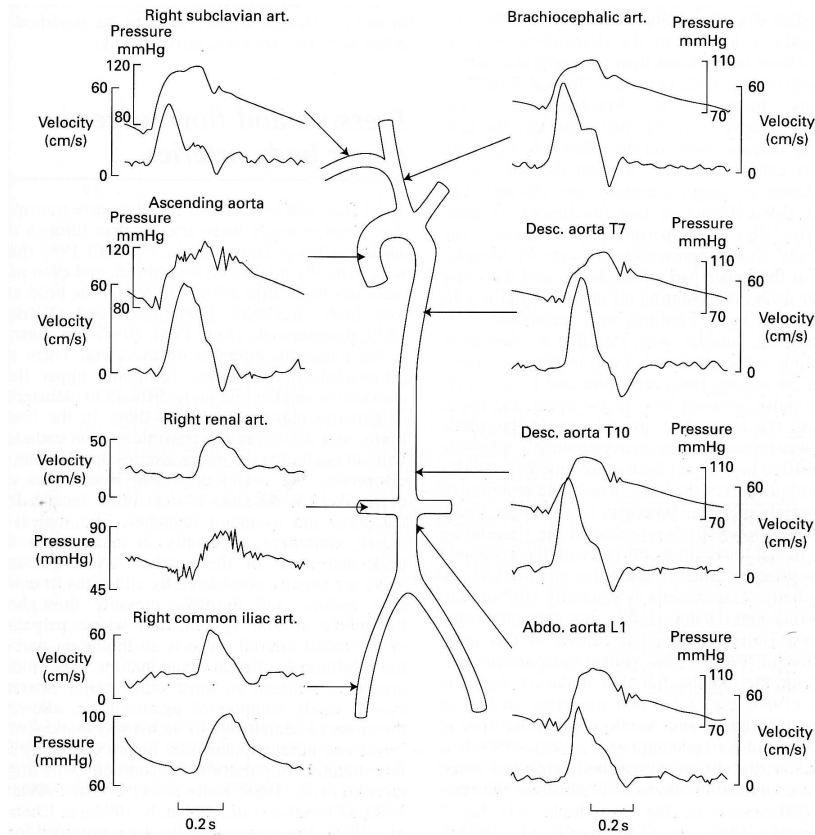
Figure 1.2: *Pressure and velocity wave forms in different arteries (Mills et. al. [26], adapted by McDonalds [31])*

nal aorta, the effect of the back travelling wave could not be observed having any essential influence on the pressure waveform in the ascending aorta. In there model for the blood flow in the aorta they divided the pressure wave into two parts, one describes the pressure as result of the Windkessel, and the part of the heart generated pressure wave. It can be seen that shape of the latter is very similar to the flow waveform when wave reflection is neglected.

A diagrammatic comparison of the behaviour of the arterial pressure and flow pulses as they travel away from the heart is given with fig. 1.2. As shown in the graphic above mean pressure falls slowly, but the pulsatile pressure variation increases until it may be double that at the root of the aorta. The flow oscillation, on the contrary, diminishes markedly. This behaviour can only be accounted for by the presence of a closed type of reflection in the
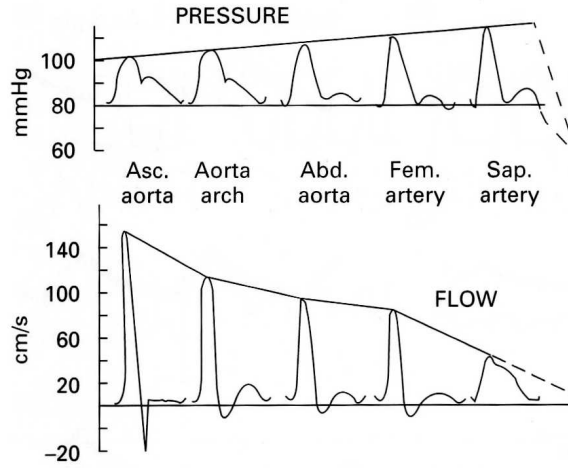
Figure 1.3: *Pressure and flow wave forms along the arterial tree (taken from McDonalds [31])*

small peripheral vessels. In the absence of reflections, damping would cause a parallel fall in pressure and flow oscillations. Subsequently, also the pressure oscillations must damp out, which takes place in the smallest arteries and proximal arterioles.

The increase in the ratio of the pulsatile pressure amplitude to that of the flow amplitude is largely determined by the increase in impedance of the low-frequency components. Additionally, the change in shape of pressure wave to that of the flow wave depends on the changes in impedance of the various frequency components in terms of their distance form the main reflection sites, since the impedance is at a minimum at one-quarter wavelength distance from these peripheral sites.

The prolonged pressure rise from wave reflection after systolic ejection has ceased leads to an augmentation of diastolic pressure and increases coronary blood flow to the myocardium without increasing left ventricular afterload. Wave reflection during diastole, therefore, appears to be highly advantageous.

In contrary to this when vessel walls become stiffer, for example in later years or through systemic hypertension, an increase in pulse wave velocity is caused what results in an early return of the reflected wave to the ascend-
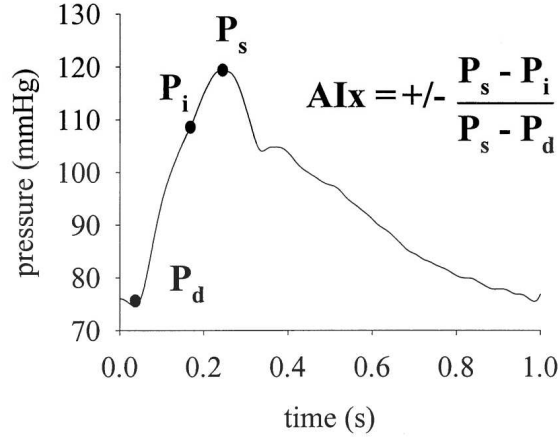
Figure 1.4: *Pressure and flow wave forms along the arterial tree (taken from McDonalds [31])*

ing aorta during ventricular ejection. Such timing is detrimental, since the augmentation caused by the reflected wave increases systolic pressure and ventricular afterload.

Thus, the so-called augmentation index, which is defined by

$$AIx = \frac{P_s - P_i}{P_s - P_d} \qquad (1.8)$$

with systolic (P_s), diastolic (P_d) and inflection pressure (P_i) is taken as a cardiovascular risk factor. (fig. 1.4). The inflection point is defined as the point when systolic ejection is over and only the reflected wave causes an increase of blood pressure.

1.2.3 Fourier Analysis

Using Fourier analysis for blood flow simulation was motivated from the theory of electrotechnical engineering, where it was is known as a quite powerful tool. Although this theory was little used before for investigating wave forms in arteries, it was finally introduced by Womersley. Using Fourier decomposition of pulse and flow waves allows to investigate the complex behaviour of non-linear distensibility and viscous effects.

McDonald gave a huge and detailed overview of Fourier analysis concerning pressure and flow waves in his fundamental book [31]. As experiments show low frequency components dominate the Fourier decomposition of waves in large arteries. Components with a frequency higher than 15 Hz can be neglected what makes its computation quite fast what leads to a high performance in computation of linear models which a huge number of segments. More details will be given later on.

Chapter 2

Fluid Mechanical Properties

"During our crossing, Einstein explained his theory to me every day, and by the time we arrived I was fully convinced he understood it."

Chaim Weizmann, 1921

The following small introduction to fluid mechanics is based on the excellent book of Acheson [1]. It should introduce into its basics and its notation to be able to understand this thesis without any foreknowledge in this topic. For further details the reader is referred to [1, 22, 37].

The flow of a fluid is described by a velocity vector

$$\boldsymbol{u} = \boldsymbol{u}(\boldsymbol{x}, t) \tag{2.1}$$

It defines the velocity at every position $\boldsymbol{x}$ for every time t. This tells us what all elements of the fluid are doing at any time, and usually finding the solution of 2.1 is the main task, what can be expected to be quite difficult. Assuming Cartesian coordinates and denoting $\boldsymbol{u}$ having components u, v, w, equation 2.1 is a convenient shortcut for

$$u = u(x, y, z, t),\ v = v(x, y, z, t) \text{ and } w = z(x, y, z, t).$$

A flow is called steady if

$$\frac{\partial \boldsymbol{u}}{\partial t} = 0$$

so that $\boldsymbol{u}$ depends on $\boldsymbol{x}$ only.

A streamline is a curve $\boldsymbol{x}(s)$ at a certain time t whereby its gradient is given by $\boldsymbol{u}(\boldsymbol{x}(s), t)$. At any particular point, a streamline has the same direction as $\boldsymbol{u}(\boldsymbol{x}, t)$ and so its following a fluid particle. Mathematically, a streamline is gained by solving

$$\frac{\mathrm{d}x/\mathrm{d}s}{u} = \frac{\mathrm{d}y/\mathrm{d}s}{v} = \frac{\mathrm{d}z/\mathrm{d}s}{w}$$

at a particular time with $x = x(s)$, $y = y(s)$ and $z = z(s)$.

It is clear that even if we have a steady flow so that $\boldsymbol{u}$ is constant at a point fixed in space, $\boldsymbol{u}$ changes as we follow any particular fluid element. This leads us to introduce the concept of *rate of change following the fluid*, with is of fundamental importance in fluid dynamics.

Rate of change "following the fluid"

Let $f(x, y, z, t)$ denote some quantity of interest in the fluid motion, for example it could be one component of the fluid velocity $\boldsymbol{u}$ or the density ρ. First, we note that $\frac{\partial f}{\partial t}$ is the rate of change of f at any fixed position in space.

In contrast to this describing the behaviour of any state variable along a path of a particle we use the *substantial derivative*

$$\frac{Df}{Dt} = \frac{d}{dt} f[x(t), y(t), z(t), t]$$

where $x(t)$, $y(t)$ and $z(t)$ are understood to change with time at the local velocity $\boldsymbol{u}$:

$$\frac{\mathrm{d}x}{\mathrm{d}t} = u, \quad \frac{\mathrm{d}y}{\mathrm{d}t} = v, \quad \frac{\mathrm{d}y}{\mathrm{d}t} = w$$

Application of the chain rule gives

$$\frac{\mathrm{D}f}{\mathrm{D}t} = \frac{\partial f}{\partial t} + u\frac{\partial f}{\partial x} + v\frac{\partial f}{\partial y} + w\frac{\partial f}{\partial z},$$

i.e.

$$\frac{Df}{Dt} = \frac{\partial f}{\partial t} + (\boldsymbol{u} \cdot \nabla)f \tag{2.2}$$

It describes the gradient of the concerned variable along a streamline. Therefore, the acceleration in a fluid at any point in space is given by

$$\frac{D\boldsymbol{u}}{Dt} = \frac{\partial \boldsymbol{u}}{\partial t} + (\boldsymbol{u} \cdot \nabla)\boldsymbol{u}$$

Remark that for steady flow equation 2.2 shows that the rate of change of f following a fluid element reduces to $(\boldsymbol{u} \cdot \nabla)f$.

Additionally,

$$(\boldsymbol{u} \cdot \nabla)f = 0 \tag{2.3}$$

defines some important stages in fluid theory, thus implies that f is constant along a streamline. But there is no information about if f is different on different streamlines. For example consider a flow in x direction and assume f to be constant in x, so that $\frac{\partial f}{\partial x} = 0$. It says that f is independent of x, but there is no information about y, z, or t.

Another important equation within the theory is

$$\frac{\mathrm{D}f}{\mathrm{D}t} = 0$$

which means that f is constant for a particular fluid element and follows directly from the definition above. It doesn't preclude that different elements might have different values of f.

For the following theory we will introduce the term of an *ideal fluid* and we will consider fluid elements with a small, but finite volume:

A fluid is said to be *ideal* as of the following properties hold:

1. It is *incompressible*, so that no finite volume element can change its volume as it moves.

2. The density ρ is a constant, the same for all fluid elements and for all time t.

3. The force exerted across a geometrical surface element $\boldsymbol{n}\partial S$ within the fluid is

$$p\boldsymbol{n}\,\partial S \qquad (2.4)$$

where the pressure $p(x,y,z,t)$ is a scalar function, independent of the normal $\boldsymbol{n}$.

Of course, there is no ideal fluid somewhere in nature, especially blood is viscous to its extent, but for our next considerations we will assume that our fluid behaves like one.

From the assumptions of the definition of an ideal fluid several consequences are implicated. First, consider a fixed closed surface S in the fluid with a unit outward normal $\boldsymbol{n}$, where fluid is entering on one side and will leave it on another. Then, the velocity component along the outward normal is $\boldsymbol{u}\cdot\boldsymbol{n}$ and the volume flowing out through a small surface element δS in unit time is $\boldsymbol{u}\cdot\boldsymbol{n}\,\delta S$, and therefore the rate fluid is leaving the volume element is given by

$$\int_S \boldsymbol{u}\cdot\boldsymbol{n}\,\mathrm{d}S$$

which must be equal to zero for an incompressible fluid and by using the divergence theorem A.2 we find

$$\int_S \nabla \cdot \boldsymbol{n} \, \mathrm{d}V = 0$$

This can be hold only for

$$\nabla \cdot \boldsymbol{u} = 0$$

what is named *incompressibility condition.*

To examine the consequence of the third condition lets consider a surface S of a finite volume. The force exerted by the surrounding fluid across any small surface element δS is given by 2.4 and the force exerted on the whole volume element is

$$-\int_S p\boldsymbol{n} \, \mathrm{d}S = -\int_V \nabla p \, \mathrm{d}V \tag{2.5}$$

if we apply the identity A.3. Assuming ∇p to be continuous it will be almost constant over a small volume δV and the force on the small volume of the surrounding fluid can be taken as $-\nabla p \, \delta V$.

The equations of Euler

Now we are in the position to study linear momentum to a small volume element δV. With the presence of gravity, the total force on our volume is

$$(-\nabla p + \rho \boldsymbol{g}) \, \delta V$$

and by Newton's second law this must be equal to mass times acceleration, i.e. to

$$\rho \, \delta V \frac{\mathrm{D}\boldsymbol{u}}{\mathrm{D}t}$$

and we obtain

$$\frac{\mathrm{D}\boldsymbol{u}}{\mathrm{D}t} = -\frac{1}{\rho}\nabla p + \rho\boldsymbol{g}$$

$$\nabla \cdot \boldsymbol{u} = 0$$

as the basic equations for an ideal fluid, known as *Euler's equations*, describing non-viscous flow of an ideal fluid.

Viscous Flow

Considering blood flow in arteries viscous effects cannot be neglected in smaller vessels. Along the vessels boundary, inviscid theory is predicting a slip of the fluid. Yet close inspection reveals that there is in fact no such slip. Instead there is a very thin boundary layer, across which the flow velocity undergoes a smooth but rapid adjustment to precisely zero. In this boundary layer inviscid theory fails and viscous effects become important.

It is obvious that the thickness of the boundary layer dominates more and more against the main part of flow the smaller the considered arteries are.

To examine viscosity consider simple shear flow, for example let the velocity u be $\boldsymbol{u} = [u(y), 0, 0]$. The fluid above some constant level y exerts stress, i.e. a force per unit area of contact on the fluid immediately below and vice verse. For inviscid flow this stress would have no tangential component, but for viscous flow this tangential component τ is typically non-zero.

If τ is proportional to the velocity gradient, i.e.

$$\tau = \mu\frac{\mathrm{d}u}{\mathrm{d}y} \tag{2.6}$$

the fluid is called to be *Newtonian* viscous. A wide range of natural fluids behave like 2.6 under "normal" conditions, also blood can be assumed to do so.

Very often the so-called *kinematic viscosity*

$$\nu = \frac{\mu}{\rho} \tag{2.7}$$

is more significant from the fluid dynamical point of view. These values can vary quite substantially with temperature, but for our applications on blood flow they can be taken to be constant, as well as we consider only constant body temperature.

For an incompressible Newtonian fluid of constant density ρ and constant viscosity μ its motion is governed by the *Navier-Stokes equations*

$$\frac{\partial \boldsymbol{u}}{\partial t} + (\boldsymbol{u} \cdot \boldsymbol{\nabla})\boldsymbol{u} = -\frac{1}{\rho}\nabla p + \nu\nabla^2\boldsymbol{u} + \boldsymbol{g} \tag{2.8}$$

$$\nabla \cdot \boldsymbol{u} = 0 \tag{2.9}$$

These differ from the Euler equations by virtue of the viscous term $\nu\nabla^2\boldsymbol{u}$, where ∇^2 denotes the Laplace operator.

No-slip Condition

Observations of real fluid flow reveals that at a rigid boundary the tangential as well as the normal component of the fluid velocity must be the same as those of the boundary itself. If we assume the boundary to be in rest, this means $\boldsymbol{u} = 0$ there. This holds for fluids of any viscosity $\nu \neq 0$.

The Reynolds Number

The Reynolds number gives a rough indication of the relative magnitudes of two terms in the equations of motions. Flows with high or low Reynolds number have quite different general characteristics. It is defined by the characteristic properties U, which denotes the typical flow speed, the characteristic length L and the viscosity ν:

$$R = \frac{UL}{\nu}$$

To understand its importants consider the derivatives of the flow velocity, e.g. $\frac{\partial u}{\partial x}$ which will be of the order U/L. Going on the derivative will change themselves of order U/L over distance of order L and the second derivative $\partial^2 u/\partial x^2$ will be of order U/L^2 and for the derivative terms in the first equations of 2.9 there holds

$$
\begin{aligned}
\text{inertia term:} \quad & |(\boldsymbol{u} \cdot \nabla)\boldsymbol{u}| = O(U^2/L) \\
\text{viscous term:} \quad & |\nu\nabla^2\boldsymbol{u}| = O(\nu U/L^2)
\end{aligned}
$$

For the ratio of the inertia and the viscous term we get

$$ O\left(\frac{U^2/L}{\nu U/L^2}\right) = O(R) \tag{2.10} $$

and the meaning of high and low Reynolds numbers becomes clear.

High Reynolds Number Flow

For high Reynoldsnumber $R \gg 1$ equation 2.10 suggests that viscous effects can be neglected and flow can be seen being in-viscous. A high Reynolds number is important over most of the flow field, but its not sufficient. In thin boundary layers where large velocity gradients occur and the viscous term in the latter equation increases. It can be shown [1] that the typical thickness δ of such a boundary layer is given by

$$ \frac{\delta}{L} = O\left(R^{-\frac{1}{2}}\right) $$

Therefore, the larger the Reynolds number, the thinner the boundary layer.

Another complication of high Reynolds number is that steady flows are often unstable to small disturbances and as a result they become turbulent. This was the original context in which the Reynolds number where defined.

Low Reynolds Numbers

Low Reynolds numbers $R \ll 1$ cover very viscous flow with special properties. In such flows there is no sign of turbulence and the flow is extremely well ordered. Furthermore, their is almost reversibility of flow. For example imagine two cylinders with golden syrup in between, the inner in rotation, the outer in rest. Considering a small volume element it will move back almost to its inertial position after the rotational force ends [1].

Viscous flow where this phenomenons became important will not considered within this thesis and so the reader is referred to literature.

Chapter 3

Haemodynamical Properties

"Marriage is like pi - natural, irrational, and very important."

Lisa Hoffman

This chapter gives an historical overview of the development of haemodynamical models and describes the key properties which are commonly used when simulating blood flow in human arteries.

During the history a lot of approaches lead to a huge amount of models by a lot of investigators. As first William Harvey (1578-1657) proved the existence of blood circulation in his work *Exercitatio anatomica de Motu Cordis* in 1628. Hundred years later Stephen Hales qualitatively described the first lumped parameter model of the arterial system in 1733 [13]. He envisioned that heart injects blood into the arterial system during systole while distending the large arteries. Furthermore he figured out that during diastole the arteries recoil and make the blood flow through the small arteries continuous. Therefore he viewed the role of the large arteries a storage device that transforms intermittent flow from the heart into a steady outflow.

Figure 3.1: *Stephen Hales, 1677-1761*

3.1 The Windkessel Approach

In the end of the nineteenth century Otto Frank conceived a practical use for this concept when he attempted the so-called Windkessel to calculate stroke volume from measured aortic pressure. Measurement of flow remained a big goal for decades until the electromagnetic flow probe was developed.

Frank related the Windkessel to represent the arterial part of the cardiovascular tree, the outflow noted to represent the arterioles and capillaries [9]. He used the principle of conservation of mass to quantify this description, where at each time t blood flow stored in the large arteries Q_{stored} is equal to the difference of inflow and outflow:

$$Q_{stored} = Q_{in} - Q_{out} \tag{3.1}$$

Then the most basic assumption of the Windkessel approach was made, namely to assume the pressure to be the same everywhere in the arterial system, which is equivalent to that the pressure and flow pulses travel with infinite velocity.

With this assumption the peripheral resistance was introduced, describing the relationship of a pressure drop across the small arteries to the flow out
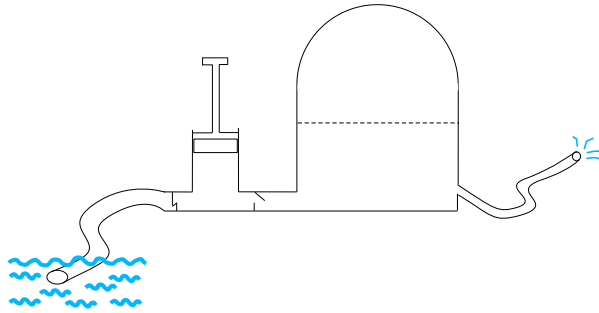
Figure 3.2: *Technical Windkessel*

of the system

$$R_w = \frac{P_{in} - P_v}{Q_{out}} \tag{3.2}$$

where P_v denotes the venous pressure. Next, the Windkessel compliance C_w describes the ability of the system to store blood which is given by the change of blood volume V caused by a change of pressure.

$$C_w = \frac{\mathrm{d}V}{\mathrm{d}P_{in}} \tag{3.3}$$

Substitution of 3.2 and 3.3 into 3.1 leads to a differential equation relating P_{in} to Q_{in}.

$$Q_{in}(t) = C_w \frac{\mathrm{d}P_{in}}{\mathrm{d}t} + \frac{P_{in}}{R_w}$$

For Frank three possible cases have to be considered for the compliance. Either C_w and R_w are both constant, both are a function of pressure or only C_w is a function of pressure. Setting Q_{in} to zero and writing the last equation in the form

$$C_w \cdot R_w = -\frac{P_{in}}{\mathrm{d}P_{in}/\mathrm{d}t}$$

he concludes that C_w is a function of pressure, which was also consistent with the observed pressure-dependent compliance of the isolated aorta.

But due the lack of possibilities of solving nonlinear equations this nonlinear description was neglected by investigators for a long time until computers made the task less difficult.

Even with pressure dependent compliance Frank's modell didn't match pressure measured from an animal and this let him to split the pressure pulse into two components, into a basic "Grundform" and an oscillating part called "Grundschwingung". His model matched the "Grundfrom", which is the pressure pulse without reflection from peripheral sites.

The real power of the Windkessel concept was not realized until Fourier Transformation was applied and it was translated into its electrical analogy. Summing up, the Windkessel approach relates flow to pressure by the arterial compliance, flow velocity was seen to be not important, which was not shared by everyone and let another school establish, the long tube school.
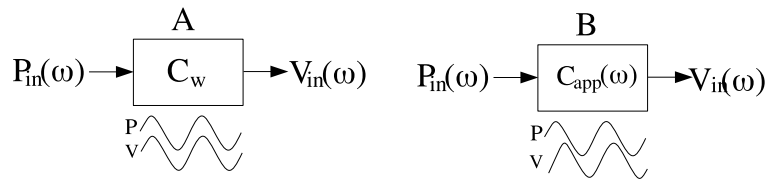

Figure 3.3: *Windkessel compliance as frequency-independent transfer function (A) and as a frequency-dependent transfer function. Here, V lags P due inertial and reflection effects.*

3.2   The Long Tube Approach

Whereas Hales and Frank saw the arterial system as a container of blood, Weber and Womersley saw it as a system transporting pressure and flow waves. Based on the observation that flow and pressure pulse waves don't rise and fall simultaneously throughout the system it was conceptualised as a uniform, infinitely long tube, so that a pulse wave produced by the heart never returns. In contrary to the Windkessel model, the focus is on wave speed velocity and this led to a long history of investigation.

This view was motivated by the observation that pressure doesn't rise and fall synchronously throughout the arterial system and a measurable time delay occurs between the pressure pulse measured at the aorta and at peripheral arteries.

In general, three equations are used to describe flow in elastic tubes: An equation of motion, an equation of continuity, and an equation describing wall properties. In the beginning of the investigation of pressure wave propagation several analytic equations were found, whereby the Moens-Kortweg formula is the most famous representative. For a thin-walled tube the pulse wave velocity c_0 is expressed as a constent value related to blood density ρ, wall thickness h, radius r and Young's modulus of elasticity E:

$$c_0 = \sqrt{\frac{hE}{2\rho r}}$$

This formula neglects effects of blood viscosity and was experimentally validated by Moens [28] but may approximate reality very well.

In a following epoch investigators started with a more formal approach and assumed the Navier-Stokes equations which were simplified to solve this non-linear partial differential equations analytically. This was the very productive time when Womersley provided a series of papers [56, 58, 57], resulting in solutions including the complex interaction of resistive and inertial forces, introduced by pulsatile flow.

3.3 The Branching Network Approach

Similar to the latter approach this approach is based on the Navier-Stokes equations by adding more and more complexity to the models. Similar to the latter method this approach is based on solving the Navier-Stokes equations with flow velocity and pressure as variables of interest. The elegant vector
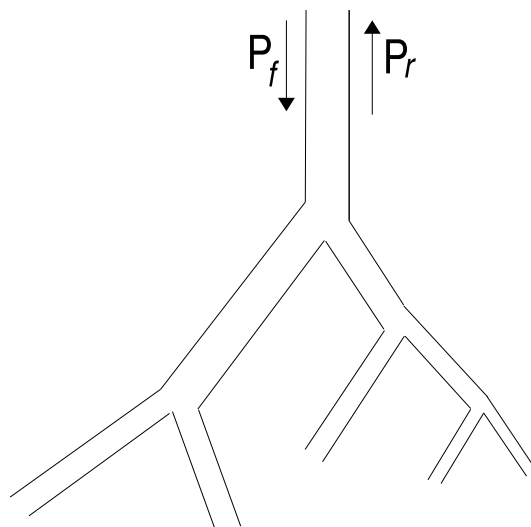
Figure 3.4: *A branching network model*

form is given by

$$\rho \frac{D\mathbf{v}}{Dt} = -\nabla P + \mu \nabla^2 \mathbf{v}$$

This relates the inertial force $\rho \frac{D\mathbf{v}}{Dt}$ to the pressure force ∇P and viscous forces $\mu \nabla^2 \mathbf{v}$.

For solving this equations analytically usually troublesome terms are neglected. Even a general solution was found by Meblin and Noordergraaf [25], the simplified less powerful approach was used by investigators. A justification of the assumption that non-linear terms are negligible was was done e.g. by Li et al. [21].

Chapter 4

Lumped Parameter Model

"Basic research is what I'm doing when I don't know what I'm doing."

Wernher von Braun

This chapter should introduce in a lumped parameter model for human blood flow which was content of my diploma thesis [19]. Based on the model from [29] a six compartment model was developed and extended with a control mechanism and the dependency of outer influences as physical stress and hydrostatical pressure. Furthermore a simulation environment for simulation of blood flow in arteries was developed which gives a control engine for the simulation of all models described in this work.

With this simple approach we gain values for heart rate, systemic blood pressure, beat volume and the peripheral resistance, averaged over one heart cycle. This is done by a mechanical two-pump model. Besides the two heart chambers also 4 other compartments are used to map the pulmonary- and systemic system, each with arterial and venous part. Furthermore a control mechanism, patterned on the natural control by the medulla and its pressure receptorsis is added to the system (refer to 4).
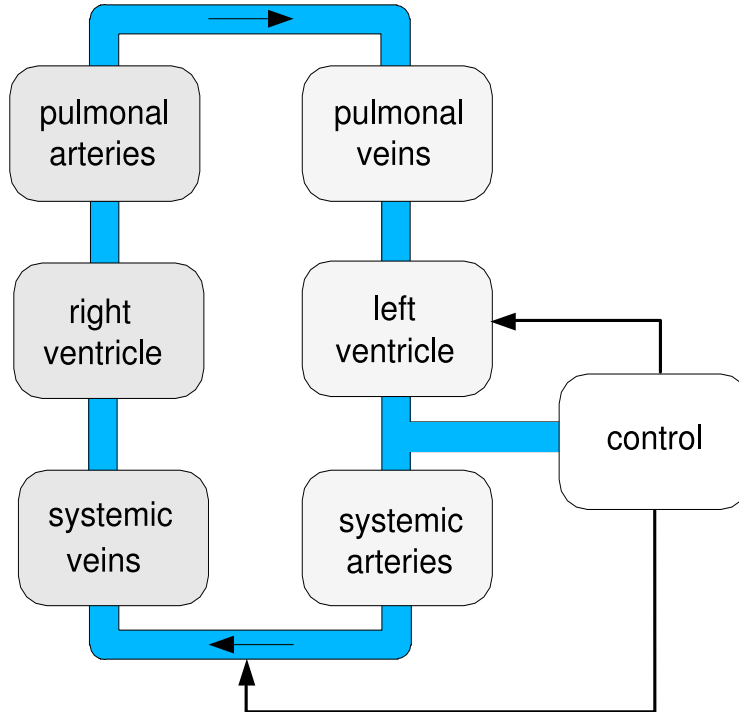
Figure 4.1: *Compartmental model scheme*

4.1 The circuit model

The compartments mathematical description is motivated through the Frank-Starling relation for the heart chambers and Poiseille's law for the compartments, describing the arteries and veins.

From the Frank-Starling relation we get that an increase of the ventricle strength k with constant arterial pressure P_A and constant end-diastolic volume V_D will increase the beat volume:

$$v_B = \frac{k}{P_A} V_D \tag{4.1}$$

On the other hand is the beat volume given by the difference of end-diastolic

and end-systolic volume

$$v_B = V_D - v_S. \tag{4.2}$$

Finally the end-systolic blood volume v_S can be written as

$$v_S = \left(1 - \frac{k}{P_A}\right) V_D \tag{4.3}$$

For the mathematical formulation of the system also the ventricle volume v_V is needed which is modeled by haemodynamic considerations. The change with time of a control volume can be written as difference of flow at discrete points x and $x + \Delta x$:

$$\frac{\partial v_V}{\partial t} = q(x, t) - q(x + \Delta x, t) \tag{4.4}$$

After determination of its Taylor series

$$q(x + \Delta x, t) = q(x, t) + \frac{\partial q}{\partial x} \Delta x \tag{4.5}$$

and substitution in equation 4.4 we get the continuity equation for flow in an elastic pipe with compliance $C = \frac{\partial v_V}{\partial p} \frac{1}{\Delta x}$

$$-\frac{\partial q}{\partial x} = c \frac{\partial p}{\partial t} \tag{4.6}$$

After taking into account the frequency dependent elasticity modulus and some equivalent transformations we get

$$b_V = \frac{c\, p_{ven} \left(1 - e^{\frac{-t_D}{CR}}\right)}{\frac{p_{art}}{k} \left(1 - e^{\frac{-t_D}{CR}}\right) + e^{\frac{-t_D}{CR}}} \tag{4.7}$$

for the beat volume, whereby t_D defines the duration of diastole. For more details the reader is referred to [48].

The mathematical description of the four remaining volume compartments is done by use of Poiseuille's law:

$$Q = \frac{\pi R^4 (P_1 - P_2)}{8\mu L} \tag{4.8}$$

The change of volume in one compartment is given by the difference of inflow and outflow

$$\frac{\mathrm{d}v_{AS}}{\mathrm{d}t} = q_{out} - q_{in}$$

whereby further on for better understanding subscripts will be used for distinguish between the systemic arterial $(_{AS})$, systemic venous $(_{VS})$, pulmonal arterial $(_{AP})$ and pulmonal venous $(_{VP})$ parts of the CVS. Variables will be written in lower case letters where we use p for pressures, v for volumes, q for flow, c for compliances and r for peripheral resistances as given by table 4.1. Constants are denoted by capitals.

After lumping the parameters in equation 4.8 to a single one, named as peripheral resistance r for the change of volume follows

$$\frac{\mathrm{d}v_{AS}}{\mathrm{d}t} = q_{out} - \frac{p_{AS} - p_{VS}}{r_A}$$

The relation between pressure and volume is given by the compliance of the arterial walls. An increased blood volume v_{AS} leads to the pressure p_{AS}, determined by the differential equation

$$\frac{\mathrm{d}p_{AS}}{\mathrm{d}t} = \frac{1}{c}\frac{\mathrm{d}v_{AS}}{\mathrm{d}t} \tag{4.9}$$

Describing all 4 compartments through this principle we gain the following

system of ordinary differential for the uncontrolled system:

$$
\begin{pmatrix} \dot{p_{AS}} \\ \dot{p_{VS}} \\ \dot{p_{AP}} \\ \dot{p_{VP}} \end{pmatrix} = \begin{pmatrix} -\frac{1}{c_{AS} \cdot r_A} & \frac{1}{c_{AS} \cdot r_A} & 0 & 0 \\ \frac{1}{c_{VS} \cdot r_A} & -\frac{1}{c_{VS} \cdot r_A} & 0 & 0 \\ 0 & 0 & -\frac{1}{c_{AP} \cdot r_P} & \frac{1}{c_{AP} \cdot r_P} \\ 0 & 0 & \frac{1}{c_{VP} \cdot r_P} & -\frac{1}{c_{VP} \cdot r_P} \end{pmatrix} \begin{pmatrix} p_{AS} \\ p_{VS} \\ p_{AP} \\ p_{VP} \end{pmatrix} + \begin{pmatrix} \frac{1}{c_{AS}} q_L \\ -\frac{1}{c_{VS}} q_R \\ \frac{1}{c_{AP}} q_R \\ -\frac{1}{c_{VP}} q_L \end{pmatrix}
$$

Value	Description
p_{AS},p_{VP},p_{VS},p_{AP}	pressure of the venous resp. the arterial part of the systemic and the pulmonal circulation
c_{AS},c_{VS},c_{AP},c_{VP}	compliances, taken to be constant
r_A,r_P	peripheral resistance of the systemic resp. pulmonal circulation
q_L,q_R	blood flow out of the left and right ventricle

Table 4.1: *Description of the used variables for the compartment modell*

4.1.1   Control of the Compartmental Model

Within the human body a lot of different mechanisms for controlling the blood pressure are known. Our considerations are restricted to the short time control by the pressure receptor as mentioned before. To add this mechanism on the model we use a negative feedback of the pressure p_{AS} with appropriate functions. These feedback functions reflect the relation between the peripheral resistance respectively the heart rate and the blood pressure, gotten through measured data. The feedback functions are realized by splines, whereby characterstic parameters like boundary points, inflection point and its gradient. These parameters can be determined from measure-
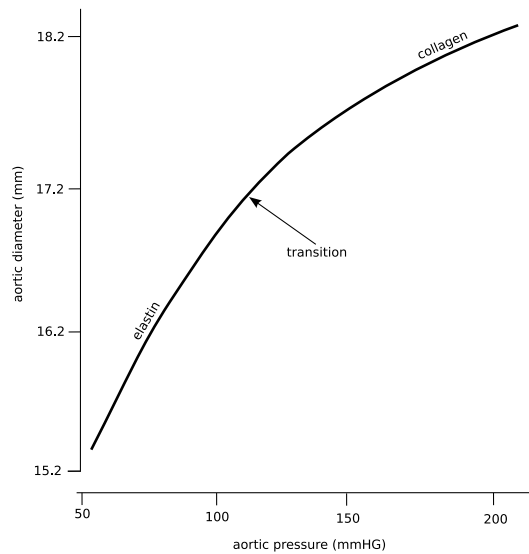
Figure 4.2: Elasticity of the aortic wall

ments easily with an optimisation method and are therefor identifiable by this way.

4.1.2   Compliance in the Controlled Model

The compliance of the arterial walls is dependent from complex mechanisms, hence the pressure as well. Therefor the assumption the compliance to be constant cannot be held. (fig. 4.2)

The compliance for the systemic and pulmonal compartments can be written as ratio of total blood volume and blood pressure:

$$c_{VS} = \frac{K_{CVS}}{p_{VS}}$$

$$c_{AP} = \frac{K_{CAP}}{p_{AP}}$$

$$c_{VP} = \frac{K_{CVP}}{p_{VP}}$$

The aortic walls consists of a thick elastic layer the aortic blood volume is changing in dependence of the blood pressure. Because of this so called

Windkessel effect the systemic volume cannot to be taken as constant. A
good approximation for this nonlinear relation between compliance CAS
and pressure PAS is given by

$$c_{AS} = CASN \cdot \left(1 - \frac{p_{ASN}^4}{1 + p_{ASN}^4} \right)$$

where $p_{ASN} = \frac{p_{AS}}{100}$ and $CASN$ set as constant.

4.2 Extended Controlled Model Considering Stress

The model described above is extended by several state variables for simu-
lating physical stress. The human physiology has two main mechanisms to
react on it. The first is a qualitative reaction and is located in the peripheral
vessels by opening or closing its circular muscles which results in a change of
peripheral resistance. It represents a very fast and energy efficient controlling
method and is modeled by a term including the stress' gradient.
The second mechanism results in increasing the heart rate and acts much
more slower, but depends on the stress quantitatively. This can be modelled
directly by the use of a transfer function of first order. But there is also an-
other mechanism with leads to decrease heartrate slowly and smoothly with
ending stress, which is represented through a transfer function of first order
as well.
Like in the original model the variables for beat volume, heart rate and pe-
ripheral resistance are represented by ordinary differential equations. The
pressure is given by flow and compliance of the vessels.

4.2.1 Peripheral Resistance

The peripheral resistance is reacting locally and fast on given stress, but its
going back to the initial value very slowly. To simulate this effect an artificial
slowly decreasing stress function was introduced:

Variables	
$\overline{r_A}$	stress dependent component of r_A
$\widehat{r_A}$	freedback component of r_A
h_{FB}	artificial smoothly decreasing stress
e_W	stress
Parameters	
T_{HFB}	time constant for h_{FB}
K_{AB}	drop rate of gradient of stress
S_{AB}	amplification factor for the gradient
R_{AG}	given gradient of the feedback function at the inflection point

Table 4.2: Model Magnitudes for the peripheral resistance

$$\dot{h_{FB}} = \{ \begin{array}{ll} -\frac{h_{FB}}{T_{HB}} + \frac{K_{HB} \cdot |\dot{e_W}|}{T_{HB}} & \text{if } \dot{e_W} < 0 \\ -\frac{h_{FB}}{T_{HB}} & \text{else} \end{array}$$

This additional differential equation describes a exponential decreasing stress function which is added on the original one, which gives as a simple way for modelling this phenomenon. The stress dependent part of the peripheral resistance can now be written as

$$\dot{\overline{r_A}} = -\frac{\overline{r_A}}{T_{HFB}} + \frac{K_{RA}}{T_{HFB}} \cdot (e_W + h_{FB})$$

4.2.2 Influence of the Hydrostatic Pressure on the Peripheral Resistance

A closer exploration of measured data gotten from a tilt table test leads to use a transfer function of first order for modelling this behaviour where the resistance is following the state of hydrostatic pressure. The oscillation at the beginning of pressure change is modelled by the use of term dependent of the differential of hydrostatic pressure what can be seen as a qualitative

control mechanism. Hence, we get

$$\dot{\overline{r_A}} = K_{RA} \cdot \dot{p_{AH}}$$

and

$$\dot{\widehat{r_A}} = -K_{PAH} \cdot p_{AH}$$

for the control of peripheral resistance in dependence of hydrostatic pressure, respectively the humans actual position.

4.2.3 Dependence of Beat Volume and Heart Rate on Hydrostatic Pressure

Due to the very fast pressure drop of the venous system caused by change of hydrostatic pressure (e.g. putting tilt table in upright position) a very abrupt decrease of beat volume is caused. In our model this is done by a linear dependence of hydrostatic pressure:

$$\dot{\overline{b_V}} = \overline{b_V} + K_{SVLH} \cdot p_{AH}$$

The same behaviour can be observed for the heart rate. Therefore its dependence on hydrostatic pressure is modeled the same way:

$$\dot{\overline{h_F}} = \overline{h_F} + K_{HRH} \cdot p_{AH}$$

4.3 Automatical Parameter Identification

For the parameter identification process a tool was developed which uses a gradient algorithm to determine the needed parameters for the control of the model based on measured data. (fig.4.4).

The identification process is divided into three parts. After a suitable pre-processing the values for the undisturbed system (without stress or influence
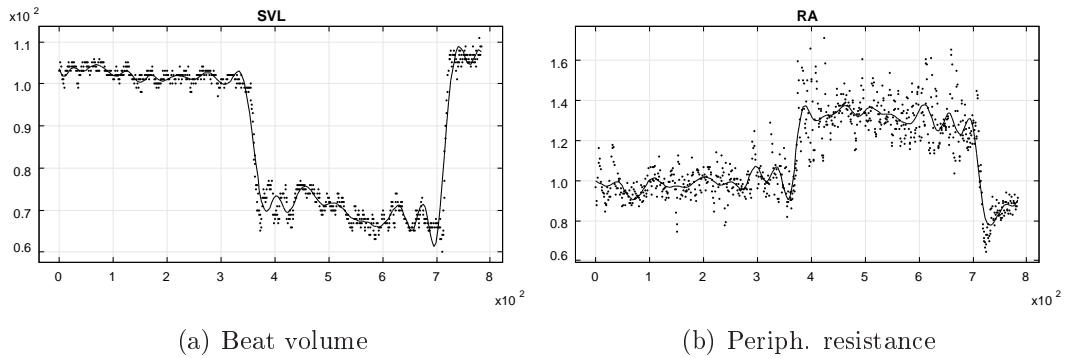
(a) Beat volume

(b) Periph. resistance

Figure 4.3: *Measure data for parameter identification*

of hydrostatic pressure) are determined. Essentially, the parameters determining the feedback functions are optimised.

Value	Description
H_{FG}	Gradient of the feedback function for the heart rate
R_{AG}	Gradient of the feedback function for the periph. resistance
C_L	Compliance of the left ventricle
C_R	Compliance of the right ventricle
K_{CVS}	Compliance of the venous system
C_{ASN}	Normed compliance

Table 4.3: *Optimised parameters of the undisturbed system*

The module approach and the use of feedback function makes it easy to identify the parameters for the different stress situations separately. After determining all necessary values for the undisturbed system, the parameters for hydrostatic pressure and the stress dependent parts can be computed.

For solving this optimisation task the class *MinConNLP* of the *JMSL Numeric Library* was used. The algorithm based on the FORTRAN subroutine, DONLP2, by Peter Spellucci. uses a sequential equality constrained quadratic programming method with an active set technique, and an alternative usage of a fully regularized mixed constrained subproblem in case of nonregular constraints (i.e. linear dependent gradients in the "working sets"). It uses a slightly modified version of the Pantoja-Mayne update
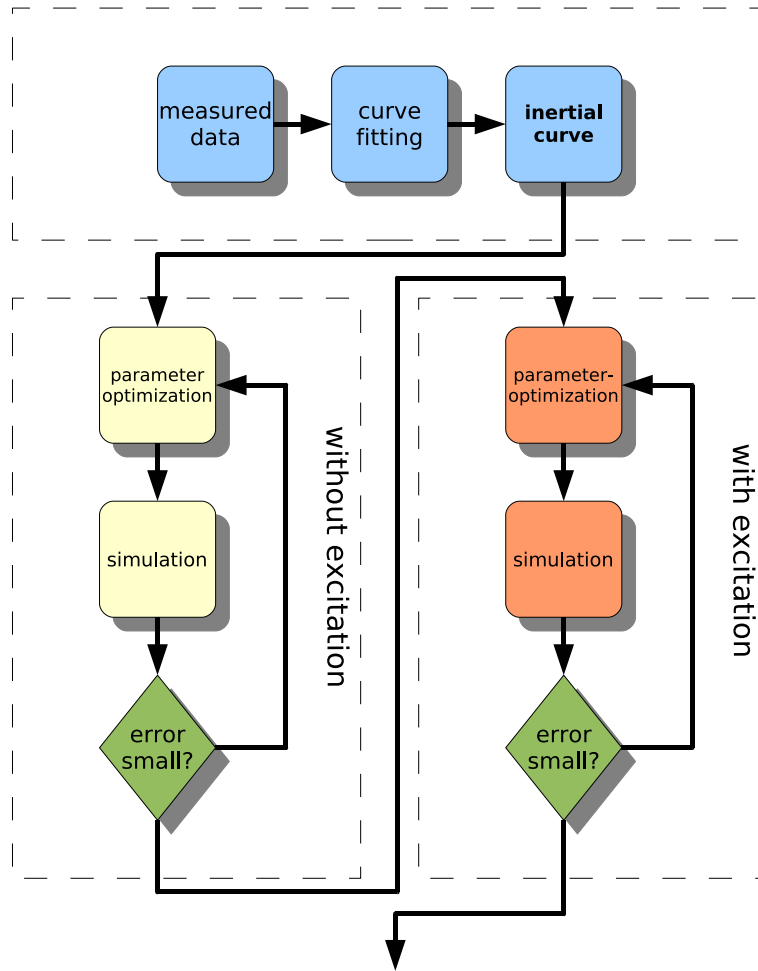
Figure 4.4: *Parameter identification scheme*

for the Hessian of the Lagrangian, variable dual scaling and an improved Armjijo-type stepsize algorithm. Bounds on the variables are treated in a gradient-projection like fashion. For more details the reader is refered to [43, 44].

Preprocessing

Before the identification process the measured data have to be averaged by curve fitting. Too many oscillations occur by the used measurement technique. Following, the time points of the beginning and the end of the distur-

bances (stress or change of hydrostatic pressure) have to be defined. Either
this was logged by the measurement tool or it has to be determined on the
measured data manually. High accuracy is not very important for this pro-
cedure, it will by higher than that of the measured data anyway.
If this is done, the needed quantities for the variables beat volume, heart rate,
peripheral resistance and mean systemic blood pressure can be computed.

Identification of the Undisturbed System

By using a gradient method which was mentioned above the parameters
concerning the mean values of the considered variables are determined. (tab
4.3). Doing this after every simulation step the goodness functional as to
be evaluated, which as a classical least square method. The algorithm is
terminating if the desired accuracy is reached or the maximum number of
iterations is exceeded.

Identification of the Parameters for the Disturbed System

Using the same procedure as before the parameters for the dependence on
outer influences are determined separately. E.g. the parameters optimised
considering hydrostatic pressure are given in table 4.4.

Name	Description
K_{PAH}	Proportional factor for pressure
K_{RA}	Proportional factor for peripheral resistance
K_{HFH}	Proportional factor for hear rate
K_{SVLH}	Proportional factor for beat volume

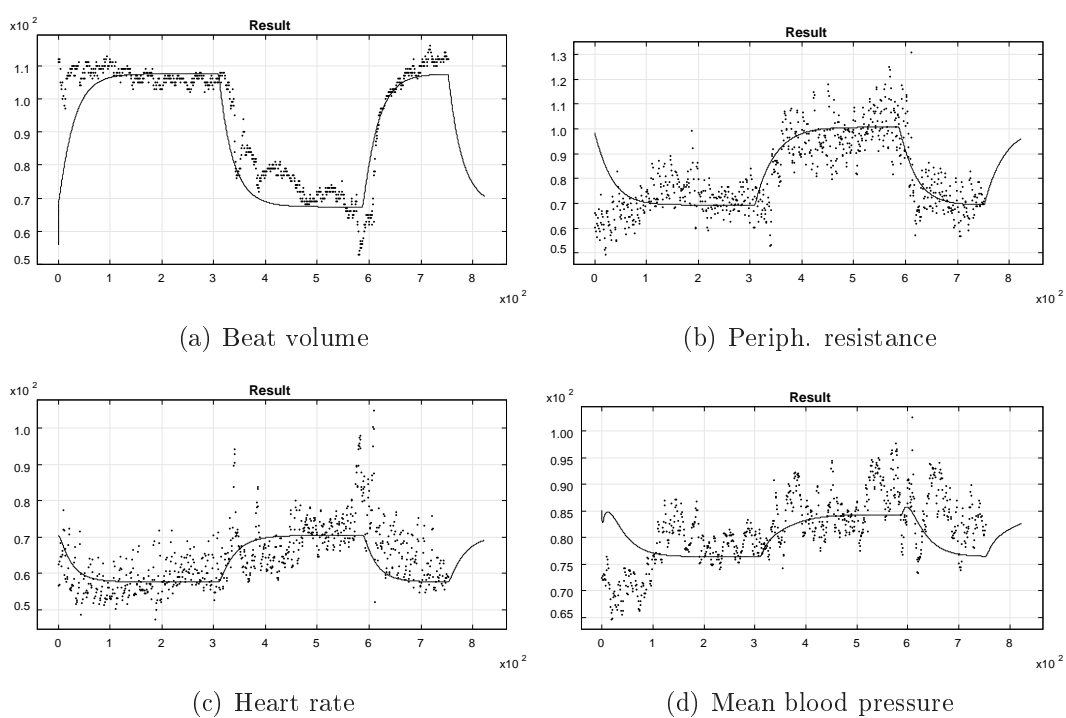**Table 4.4:** *Optimised parameters considering change of hydrostatic pressure*

(a) Beat volume

(b) Periph. resistance

(c) Heart rate

(d) Mean blood pressure

Figure 4.5: *Simulation of a tilt table test with identified parameters*

Chapter 5

One Dimensional Linearised Model

"In the 19th century fluid dynamicists were divided into hydraulic engineers who observed what could not be explained, and mathematicians who explained things that could not observed."

Sir Cyril Hinshelwood

The concept or circulation of blood was established by William Harvey in 1628. Since then numerous attempts have been made at gaining insight into the physical relations between the phenomenons being observed in the complicated anatomical structure of the circulatory system. Then, the fact that the intermitted outflow of the left ventricle is more a steady one, was recognised by Hales in 1733. He described the arterial system as a single elastic chamber which became known as Windkessel model, introduced by Frank [9] in 1899.

In the early fifties of the 20th century McDonald [23, 24] showed with help of rabbits that there is a reversal blood flow in larger arteries. Further more Helps and McDonald [17] showed a phase-lag between pressure gradient and flow somewhat analogous with the phase-lag between voltage and current in a conductor carrying alternating current. Based on these results, Womersley

[56] used the similarities with the theory of the distribution of alternating current in a conductor of finite size.

First, he considered the problem in circular tube when the pressure gradient is known. For a tube with length, filled with a fluid of viscosity μ the equation of motion of the liquid assumes

$$\frac{d^2w}{dr^2} + \frac{1}{r}\frac{dw}{dr} + \frac{p_1 - p_2}{\mu l} = 0 \qquad (5.1)$$

where w denotes the longitudinal velocity of the fluid and r the distance of the fluid element from the axis of the tube.

The solution of this first simple approach with constant pressure gradient $p_1 - p_2$ is

$$w = \frac{p_1 - p_2}{4\mu l}(R^2 - r^2) \qquad (5.2)$$

whereby R is the radius of the tube.

5.1 Observations

At the beginning of the cardiac ejection phase (systole), the pressure rises at the entrance of the aorta and a blood volume of about 80ml is ejected. Because of the vessel elasticity the pressure distends it locally. Then it contracts again and the next segment is caused to extend and so on. In fact, a wave is generated and propagates downstream, where the restoring force is provided by the elasticity of the vessel wall.

This propagation can easily be seen on measured data, more over there are three phenomenons which can be observed: First, the amplitude of the pressure wave increases when the wave propagates, second, one can observe a *steepening* of the wave front and third, the wave form of the flow velocity has another shape than the pressure wave. These phenomenons, as will be shown later, cannot be explained by a simple linear theory.

5.2   A First Simple Approach

As a first approach let us study a very simple and direct approach of mod-
elling blood flow in arteries. Therefore we begin considering an infinitely long,
straight, horizontal elastic tube with uniform undisturbed cross-sectional area
A_0 and uniform external pressure p_e, containing an inviscid incompressible
fluid of constant density ρ which is initially at rest. Further on we analyse
just disturbances with a wave length much greater than the tube diameter, so
that the time-dependent internal pressure can be taken to be a function only
of longitudinal coordinate x and time t. Because we want a one-dimensional
model we denote the disturbed cross-sectional area by $A(x,t)$ and the fluid
velocity by $u(x,t)$, which is intermitted over the cross-section.
The governing classical equations are those representing conservation of mass,
conservation of momentum and elasticity. By considering the rate of change
of volume of a thin slice of the tube, we gain the equation for conservation
of mass by

$$\frac{\partial A}{\partial t} + \frac{\partial}{\partial x}(Au) = 0 \tag{5.3}$$

The momentum equation by Euler is given by

$$\frac{\partial u}{\partial t} + u\frac{\partial u}{\partial x} = -\frac{1}{\rho}\frac{\partial p}{\partial x} \tag{5.4}$$

and the elasticity for our simple approach is modeled by the means of a so
called *tube law*, relating transmural pressure difference to local cross-sectional
area

$$p - p_e = \tilde{P}(A) \tag{5.5}$$

whereby $\tilde{P}$ is a function like in figure 5.1.
Now let us consider small amplitude disturbances such that u is small and

$$A = A_0 + A', \quad p - p_\epsilon = \tilde{P}(A_0) + p' \tag{5.6}$$

where $|A'| \ll A_0$, $|p'| \ll \tilde{P}(A_0)$. After substituting into the equations and neglecting all terms nonlinear in small quantities, we can eliminate u and A' to obtain the following single equation for p':

$$\frac{\partial^2 p'}{\partial t^2} = c^2(A_0)\frac{\partial^2 p'}{\partial x^2} \tag{5.7}$$

where

$$c^2(A) = \frac{A}{\rho}\frac{\mathrm{d}\tilde{P}}{\mathrm{d}A}$$

Equation 5.7 denotes the well known wave equation which describes wave propagation with small amplitude disturbances along the tube in either direction, but without change of shape, with speed $c_0 = c(A_0)$. The general solution of equation 5.7 is given by

$$p' = f_1\left(t - \frac{x}{c_0}\right) + f_2\left(t + \frac{x}{c_0}\right) \tag{5.8}$$

where f_1 and f_2 are arbitrary functions, whereby f_2 equals zero if we have a wave propagation in $+x$ direction only.

If we suppose the validity of the Moens-Korteweg wave speed, given through

$$c_0 = \left(\frac{Eh}{\rho d}\right)^{\frac{1}{2}} \tag{5.9}$$

which Young's modulus E, wall thickness h and diameter d for the vessels made of a homogeneous and isotropic Hookean solid material.Comparing this equation with measured data shows us a good approximation with a predicted value of $5ms^{-1}$ for the wave speed in the ascending aorta, rising to about $8ms^-1$ in more peripheral arteries.

This simple theory is very successful at establishing the mechanism of wave propagation, involving only wall elasticity and blood inertia as well as predicting the wave speed.

But on the other hand this theory predicts no change of shape of wave-form as it propagates and the velocity wave-form is of the same shape, different
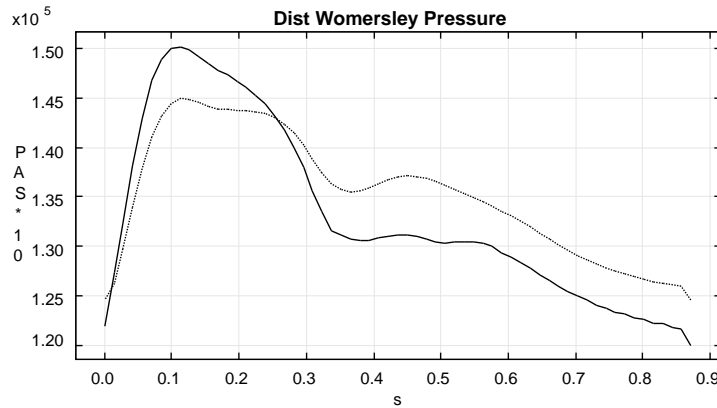
Figure 5.1: *pressure waves in ascending aorta and femoralis*

to that we find considering measured data.

Hence, the theory must be modified to account for all these effects which will be discussed below. In figure 5.1 one can observe the effects mentioned before.

5.3   The Concept of Impedance

In the simple models for simulation of the cardiovascular system a steady flow is assumed and all the properties are mean values of a cardiac cycle. For a more detailed study this assumption is no more valid cause the pulsatile behavior of pressure and flow is typical.

For the simple models the Ohmian law, $Q = \frac{P}{R}$, is taken to describe basic flow concerning the arterial resistance against the flow, generated by wall friction and by the small arteries. This law is also valid for pulsatile flow and leads to the frequency dependent variant of resistance, namely impedance.

For easier understanding we will introduce Fourier series for dividing flow, pressure and therefore impedance curves into terms of Fourier series.

We divide impedance into four different kinds, dependend on its measure point [31]:
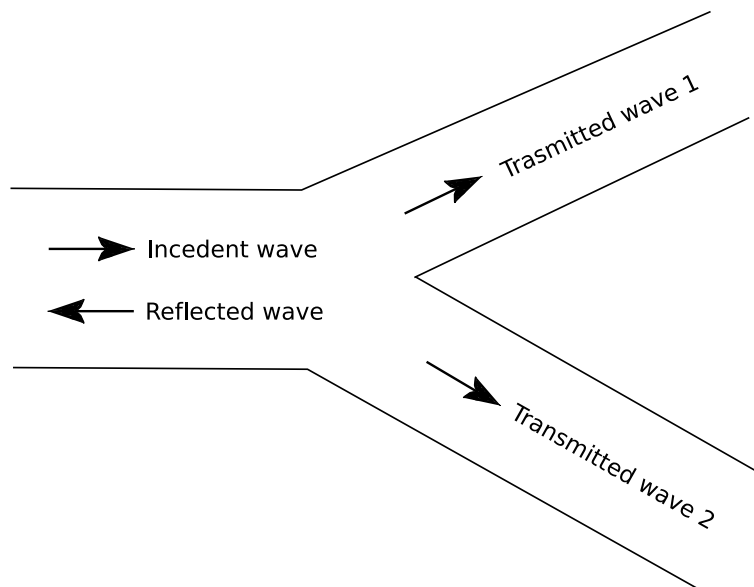
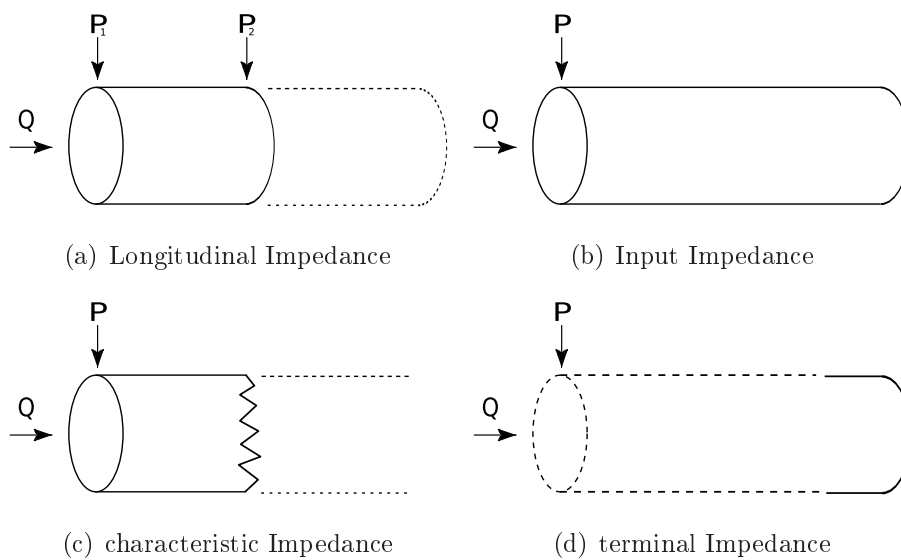**Figure 5.2:** *Wave transmission in bifurcations*

(a) Longitudinal Impedance

(b) Input Impedance

(c) characteristic Impedance

(d) terminal Impedance

Figure 5.3: *Definition of Impedance*

Longitudinal Impedance

The longitudinal impedance of a certain segment of the tube is defined by the ratio of the pressure gradient and its flow. It is not influenced by wave reflection and defines the complex analogon to the static resistance resulting from the tubes physical parameters.

Input Impedance

The input impedance measured at the systems entry gives its whole impedance and is influenced by all geometrical and physical parameters. In our applications it means the impedance at the aortic root or at the root of any subtree.

Characteristic Impedance

Whereby longitudinal and input impedances can be measured, this is not true for characteristic and terminal impedance. But they have great theoretical relevance and will be used in further considerations.

Characteristic impedance determines impedance without influence of wave reflection and is equivalent to the input impedance of a tube of infinite length. Although there is no (pulsatile) flow without reflection in nature, it is useful to consider only the non-reflective parts of waves, e.g. through filtering terms of high frequency.

Terminal Impedance

The resistance of arterioles and capillar vessels are described by the terminal impedance on peripheral segments of the vascular tree. The properties of arterioles and capillar vessels are almost frequency independent and the impedance results in a pure resistance. and the terminal impedance is therefore defined as ratio of mean pressure and mean flow.

The terminal impedance is a bit smaller than the total peripheral resistance which can be measured at the aorta. This is caused by the pressure drop along the arterial tree.

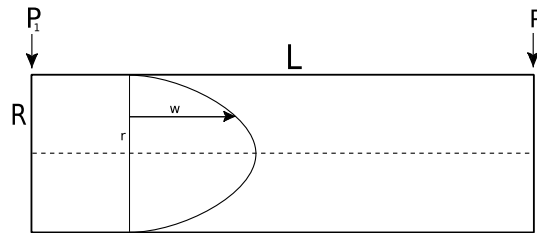## 5.4 Equation of Motion when the Pressure Gradient is Known

Figure 5.4: *Steady flow in a straight tube*

Folowing Womersley [56] let as now assume to have a circular symmetric tube of length l and radius R which is filled with a viscous fluid of density ρ and viscosity μ. Furthermore, let p_1 denote the pressure at the inflow and p_2 the pressure on the outflow of the tube with consant pressure drop $p_1 - p_2$.. For the longitudinal velocity w of the fluid with distance r from the longitudinal axis the equation of motion leads to

$$\frac{\mathrm{d}^2 w}{\mathrm{d}r^2} + \frac{1}{r}\frac{\mathrm{d}w}{\mathrm{d}r} + \frac{p_1 - p_2}{\mu l} = 0 \tag{5.10}$$

Assuming a constant pressure drop $p_1 - p_2$ its solution is given through

$$w = \frac{p_1 - p_2}{4\mu l}(R^2 - r^2)$$

which leads to a parabolic velocity profile as shown in figure 5.4.

If we take the pressure gradient not constant, a term of viscosity $\frac{1}{\nu}\frac{\partial w}{\partial t}$ occurs on the right side of equation 5.10. Lets assume the pressure gradient to be

periodic in time and the pressure term be

$$\frac{p_1 - p_2}{\mu l} = A\mathrm{e}^{int}$$

with frequency

$$f = \frac{n}{2\pi}$$

Since periodic functions can be written as sum of periodic terms we can write the equation of motion as

$$\frac{\mathrm{d}^2 w}{\mathrm{d}r^2} + \frac{1}{r}\frac{\mathrm{d}w}{\mathrm{d}r} - \frac{1}{\nu}\frac{\partial w}{\partial t} = A\mathrm{e}^{int} \tag{5.11}$$

Expecting the flow to be periodic as well, we substitute w in the latter equation by

$$w := u\mathrm{e}^{int}$$

whereby u is a function of r only, we get

$$\frac{\mathrm{d}^2 u}{\mathrm{d}r^2} + \frac{1}{r}\frac{\mathrm{d}u}{\mathrm{d}r} - \frac{in}{\nu}u = -\frac{A}{\mu} \tag{5.12}$$

or even

$$\frac{\mathrm{d}^2 u}{\mathrm{d}r^2} + \frac{1}{r}\frac{\mathrm{d}u}{\mathrm{d}r} + \frac{i^3 n}{\nu}u = -\frac{A}{\mu} \tag{5.13}$$

The solution of equation 5.13 can be found in literature and is given in closed form through

$$u = +\frac{A}{\rho}\frac{1}{in}\left\{1 - \frac{J_0\left(r\sqrt{\frac{n}{\nu}}i^{\frac{3}{2}}\right)}{J_0\left(R\sqrt{\frac{n}{\nu}}i^{\frac{3}{2}}\right)}\right\}$$

where $J_0(xi^{\frac{3}{2}})$ denotes the Bessel function of 0-th order.

The term

$$\alpha := R\sqrt{\frac{n}{\nu}}$$

in the last equation is called *Womersley number*, and was described in the last chapters.

For more convenience the equation is usually written in terms of modulus and phase, which coincides to the polar representation of complex numbers. Assuming that the pressure gradient is known, which will not be true in general, we may write the equation of flow as follows

$$w = +\frac{A}{\rho}\frac{1}{in}\left\{1 - \frac{J_0\left(\alpha y i^{\frac{3}{2}}\right)}{J_0\left(\alpha i^{\frac{3}{2}}\right)}\right\}e^{int}$$

where we substituted with $y = \frac{r}{R}$.

In general the pressure gradient will not be known and hence more complex modells have to be considered. The complete mathematical description for flow with unknown pressure gradient is given by the Navier-Stokes equations. In the following chapter the set of Navier-Stokes equations will be linearised for application on small blood vessels. This approximation will also be used in the larger arteries later.

5.5 Bifurcations

5.6 Model for smaller arteries

Based on the works of Womersely[56, 58] and Pedley[34] Olufsen[32, 33] developed a model for simulation of streams in small arteries. Starting from the equations given above their was added another relation for modelling the wall dilatation based on the continuity equation.

Similar to the model of Womersley, flow is described by continuity equation,

whereby volume flow denotes

$$Q = \int_0^a w_r 2\pi r dr \tag{5.14}$$

Here, w_r is the velocity in longitudinal direction. For a detailed derivation please refer to [33, 32, 34].

The solution is found by Bessel equation, which results from linearisation of the axis-symmetric Navier-Stokes equations and combination with equations describing the motion of the vessel wall and given by

$$w_r = \frac{p_c k'}{c_0 \rho} \left(1 - \frac{J_1(r w_0 / r_0)}{J_0(w_0)} \right) \tag{5.15}$$

where r_0 is the undisturbed vessel radius, ρ the blood density, p_c an integration constant, $k' = \frac{c_0}{c}$ the complex wave propagation velocity where $c_0 = Eh/2r_0\rho$ the Moens-Korteweg wave-propagation velocity. J_0 and J_1 denote the zeroth and first order Bessel functions.

Finally, integration over the cross-sectional area yields

$$Q = \frac{A_0 p_c k'}{c_0 \rho} (1 - F_J) \tag{5.16}$$

where A_0 is the undisturbed cross-sectional area with the shortcut

$$F_J(w) = \frac{2 J_1(w_0)}{w_0 J_0(w_0)} \tag{5.17}$$

If we denote the pressure gradient be

$$\frac{-i\omega p_c}{c} = \frac{\partial P}{\partial x}$$

we get for the momentum equation

$$iwQ = -\frac{A_0}{rho} \frac{\partial P}{x} (1 - F_J) \tag{5.18}$$

5.6.1 Continuity and State Equations

The continuity equation in one dimension is covered by

$$\frac{\partial A}{\partial t} + \frac{\partial q}{\partial x} \tag{5.19}$$

which can be written as

$$iwCP + \frac{\partial Q}{\partial x} = 0 \tag{5.20}$$

in the frequency domain after applying Fourier transformation.

For a further relation of the three unknowns pressure P, flow Q and cross sectional area A we consider an approximation for the compliance, the needed state equation when considering elastic walls:

$$C = \frac{dA}{dp} = \frac{3A_0 a}{2Eh} \left(1 - \frac{3pa}{4Eh}\right)^{-3} \approx \frac{3A_0 a}{2Eh} \tag{5.21}$$

After differentiation and integration of the equations we gain

$$Q(x, \omega) = a\cos(\frac{\omega x}{c}) + b\sin(\frac{\omega x}{c}) \tag{5.22}$$

$$P(x, \omega) = i\sqrt{\frac{\rho}{CA_0(1 - F_J)}} \left(-a\sin\left(\frac{\omega x}{c}\right) + b\cos\left(\frac{\omega x}{c}\right)\right) \tag{5.23}$$

Our goal is now to use this description of blood flow in arteries for computing its impedances, which can be done in both directions, respectively from proximal to distal or vice verse. If we reformulate the equations 5.22 and 5.23 we can write the impedance for the proximal end of an arterial segment with respect to ins distal impedance as follows:

$$Z(0, \omega) = \frac{ig^{-1}(b\cos\frac{\omega L}{c} - a\sin\frac{\omega L}{c})}{a\cos\frac{\omega L}{c} + b\sin\frac{\omega L}{c}} \tag{5.24}$$

where

$$g = \sqrt{\frac{CA_0(1 - F_J)}{\rho}}, \, a = Q(0, \omega) \text{ and } b = -iP(0, \omega)g$$

5.7 Goal and Investigations

The first idea of using this linearised approach was to gain hints of how to choose the parameters for Windkessels, used in the non-linear model as termination conditions, described in the following chapter.

Doing this, we were trying different linearised approaches based on the one dimensional Navier-Stokes equations. In literature several models were developed by a lot of investigators, considering a different level of details of the natural process of flowing blood. Each of them guarantees fast computability, what is a key feature for our application where we want to apply such models for determining boundary data in every time step of computation.

During the simulation process pressure and flow wave forms are computed where suitable initial and boundary data are given. Several different simulation scenarios are possible, which are described below. It is also shown that the linearised model is also suitable for the computation of flow and pressure waveforms by itself also for larger arteries, not only for the small ones for which it was developed. At least the model can be used for parameter identification where the quasi-linearity is a great advantage especially in the case of parameter space of high dimension what is true for most of biological models respectively for blood flow in the arterial bed.

Given Flow and Pressure Forms

The difficulty of using flow and pressure as initial data at the same time is to get suitable measured data. One the one hand all measured data contains errors, on the other hand it is not always possible to get requisite data from

measurement. E.g. it is very difficult to get synchronous measured data of flow and pressure wave forms.

In our experiment the following measurement techniques were used:

- Flow wave form from ultrasound measurement

- Pressure wave form from SphygmoCor© device

The latter measures the pressure wave form at the A. radialis and tries to compute the wave from at the aortic root. As first the quality of the central wave from depends on a lot of different factors, as second, only wave forms and not the quantitative pressure is gained. Central systolic and diastolic pressure must be guessed another way.

Given Impedance and Flow

The use of given pressure wave form is seen to be not optimal and the next approach is to use impedance instead, although it might be more difficult to get measured data. Two methods for prescribing impedance for simulation of blood flow in the arterial tree are figured out:

- Prescribing of the total peripheral resistance which can be determined indirectly with e.g. impedance cardiography and computation of the complex impedance using a replacement model (Windkessel)
  Indeed, it seems that this method underestimates the total peripheral resistance and so the quality of the impedance gained artificial to a certain extend has to be validated.

- Another approach is backward computation of impedances by help of the model described before with prescribing impedances at the peripheral arterial segments. To go around the problem of how to get data for prescribing impedances at the peripheral segments Olufsen[33] suggested an alternative method which computes impedances from small arteries, starting at the arterioles where the resistance (there is only pure resistance in this small vessels) can be assumed to be zero.
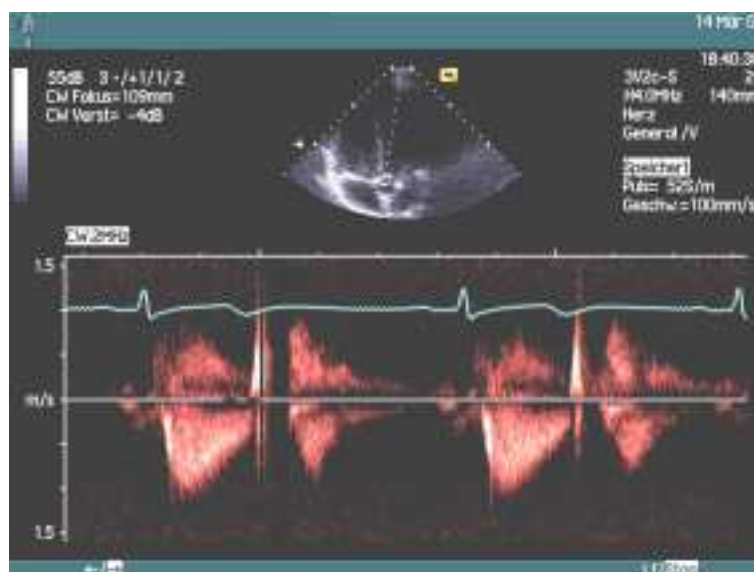
Figure 5.5: *Ultrasound measurement for the flow velocity at the aortic root*

Backtracing using Measured Data

The disadvantage of the method of Olufsen is that the model considers only the radius of the terminal segment and two parameters determine the overall behaviour of the structured tree which is generated as a replacement model for the small arteries. It doesn't take into account the humans physiological parameters and it would need some efforts to fit the model to measured data. Some optimisation method might solve this problem.

Instead, we used flow and pressure wave forms can be used to compute impedance in peripheral segments. It would be a really good method if synchronous measured data from different sites of the arterial tree would be available. Unfortunately this is not the case and this leads to a lot of problems.

First, the pressure and flow wave forms are in different time scale and the phase shift of them is of big relevance. Therefore, it is necessary to convert data to match the phase shift which is gained by comparison of the measured wave form with the synchronous measured ECG signal. This is a time consuming task which is hard to automate because the ultrasound measurement

is available only in image format and the quality of measurement varies very much and has to checked by hand.

Second, another problem occurs when matching together two impedances gained from measurement at any bifurcation. Usually the data on different sites represent different heart cycles and also the pulse wave velocity differs. Although we fitted the data before to its corresponding phase delay, this delay may differ from heart cycle to heart cycle and the resulting pressure and flow wave forms may be unrealistic. So datasets with matching ECG signals have to be chosen to keep the synchronisation error small.

5.8   Extended Model for Smaller Arteries

In the model described before investigated by Womersley[57] and used by McDonald[31] lacks of the consideration viscoelasticity. Viscoelasticity of the arterial walls results in a phase shift of treated forces and the resulting displacement of the vessel wall. This phenomenon can be considered by using the so-called dynamic Young modulus E_d[4],

$$E_d = E + i\omega\eta_w \tag{5.25}$$

where η_w denotes the viscosity of the wall

Considering pulse wave propagation, the viscoelastic properties of the vessel walls are characterised by the tangent of the angel ϕ of phase shift of current pressure and local displacement of the corresponding wall [3, 49, 54].

$$\phi = \tan^{-1}\left(\frac{\omega\eta_w}{E}\right) \tag{5.26}$$

Using this, a factor $\cos(\phi/2) + i\sin(\phi/2)$ is added to the equations in the section before.

The next step is to split impedance into a characteristic impedance, which is determined by the mechanical properties of the concerning arterial segment only, and the terminal impedance, which depends on the structure of the

following vascular tree.

Hence, the characteristic impedance is for any arterial segment is described with its wave transmission coefficient, which is given by the mechanical properties of blood and the vessel walls, the input impedance, a distribution factor and the phase velocity. By help of transmission line theory, coming from electrotechnical engineering, the reflexion coefficient is given by

$$\Gamma = \frac{Z_T - Z_0}{Z_T + Z_0}$$

where Z_T denotes terminal and Z_0 characteristic impedance of any segment.

$$Z = Z_0 \frac{1 + \Gamma \mathrm{e}^{-2\gamma l}}{1 - \Gamma \mathrm{e}^{-2\gamma l}} \tag{5.27}$$

$$\frac{p(l)}{p(0)} = Z_0 \frac{1 + \Gamma}{\mathrm{e}^{\gamma l} + \Gamma \mathrm{e}^{-\gamma l}} \tag{5.28}$$

Chapter 6

One Dimensional Nonlinear Model

"Man is the only creature that seems to have the time and energy to pump all his sewage out to sea, and then go swimming in it."

Miles Kington

Based on the one-dimensional Navier-Stokes equations for flow in axis-symmetric elastic tubes of an incompressible fluid a model for simulation of blood flow in arteries was developed. The focus hereby is on the larger arteries, which means that only vessels with an inner diameter from 50mm down to 1mm approximately are considered. For smaller arteries the model would not be valid anymore cause of several assumptions, made on the physical properties of blood. In detail, the blood cannot be taken to be homogeneous in small arteries because the red blood cells have a size of the same scale as the vessel diameters. Wibmer [55] has implemented the model with help of finite volume methods in C++. This model was coupled to the controlled parameter model described in chapter 4 to get a fully controlled model for blood flow in human arteries. In this chapter only a basic overview is given,

under special consideration of the relevant parts for this work. For further
details please refer to [55] and references therein.

6.1 Model Equations

The basic equations solved within the models are given in the (A, Q) formu-
lation where $A = A(x,t)$ denotes the cross sectional area and $Q = Q(x,t)$
the volume flow. Considering mass and momentum balance leads to

$$A_t + Q_x = 0 \tag{6.1}$$

$$Q_t + \frac{\partial}{\partial x}\left(\alpha\frac{Q^2}{A} + p\right) = K\frac{Q}{A} \tag{6.2}$$

and a state equation giving a relation between the cross sectional area and
the blood pressure. In literature, several relations for the state equation can
be found, one is given below.

Most of equations for describing wall-pressure relations assume linear elastic-
ity and are based on Hook's law. This let the pressure be a concave function
of the cross sectional area. The elastic nature of arteries is mainly determined
by the distribution of elastin and collagen in the vessel wall, which differs
from the proximal to the distal vessels. More precise, in the proximal aorta
elastin specifies its elastic behaviour while it is collagen in the periphery.
Concerning the higher elastic modulus of collagen the stiffness of the walls
increases in the distal arteries. Also collagen plays an important role in the
vessel wall elasticity. Since the transmural pressure increases, collagen fibres
determine the stiffness, whereby at low pressure it is mainly determined my
elastin fibres. This results in a nonlinear pressure dependent elastic modulus.
A simple state equation was presented by Raines [39]:

$$p(A) = p_0 e^{E_p(\frac{A}{A_0} - 1)} \tag{6.3}$$

Here, E_p is the pressure-strain elasticity modulus by Peterson et. al [36]. For
more details the reader is recommended to refer to [31] and references therein.

For the given It can be easily shown that $\frac{\partial p}{\partial A} > 0$ and $\frac{\partial p^2}{\partial^2 A} > 0$ and 6.3 is source for other simple concave equations by using Taylor polynomials of arbitrary order.

Additionally the wave velocity is given by

$$c = \sqrt{\frac{Ap_0}{\rho K A_0} e^{E_p(\frac{A}{A_0} - 1)}}$$

and its derivative with respect to A is positive.

Linearising equation 6.3 we get

$$p(A) = p_0 \left(1 + E_p \left(\frac{A}{A_0} - 1 \right) \right)$$

and

$$c(A) = \sqrt{\frac{Ap_0 E_p}{A_0 \rho}}$$

6.1.1   Bifurcations

Due to the reduction to one dimension bifurcations are not really handled by this approach. For a detailed description a three-dimensional consideration would be necessary. For our needs it is enough to assume branches as one dimensional points. Mass and momentum conservation is assumed and branches can be computed easily. For one dimensional computation this assumptions are suitable and used by a lot of authors.

6.1.2   Termination Conditions

On every modeled terminal segment of the arterial bed a terminal condition is necessary. Here, the well known Windkessel is used to model the network of small arteries, arterioles and capillaries. This model, taken from the theory of electrical circuits, consists of two resistances R_1 and R_2 and a capacity C.
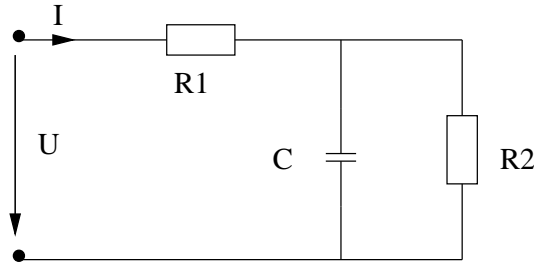
Figure 6.1: *Electrical analogon to the Windkessel*

The sum $R_1 + R_2$ defines the total peripheral resistance of the arterial network and C stands for the compliance, the distensibility of the vessel walls. With help of such Windkessels the behaviour of the small vessels can be modeled in an appropriate manner. But, for each Windkessel (25 in our case) there are 3 parameters which have to be identified by measured data, what can be expected to be a difficult task.

The frequency dependend impedance, generated by a Windkessel, is given by the equation

$$Z(\omega) = \frac{R_1 + R_2 + i\omega C R_1 R_2}{1 + i\omega C R_2} \tag{6.4}$$

In the sense of fluid mechanics the (input) impedance is the ratio of blood pressure $p(t)$ to volume flow $Q(t)$, which matches very well with the impedance produced by a Windkessel. Hence, Windkessels are a good choice for terminations within our model.

For computation we transform the equation above into the time domain and we gain an ordinary differential equation of the flow-pressure relation of a Windkessel:

$$\frac{\mathrm{d}Q(l,t)}{\mathrm{d}t} - \frac{1}{R_1}\frac{\mathrm{d}p(l,t)}{\mathrm{d}t} = \frac{p(l,t)}{R_1 R_2 C} - \left(1 + \frac{R_1}{R_2}\right)\frac{Q(l,t)}{R_1 C} \tag{6.5}$$

6.1.3 Parameter Identification for Windkessels

As simple the Windkessel model seems to be handle as difficult it is to determine its parameters. Due the impossibility of extracting the Windkessel data from measurements directly the use of replacement models is necessary. For each terminal segment three parameters have to be determined. From measured data only the total peripheral resistance, measured at the aortic root, is available. Olufsen [32] suggested the use of the linearised Womersley solution of the Navier-Stokes equations to solve it for a structured tree of small arteries with a zero terminal condition to determine its root impedance, which can be used as terminal impedance for the tree of large arteries. Due the definition of the structured tree the terminal impedance is mainly given through the radius of the terminal vessel, which cannot to be taken as valid for all segments. E.g. for the terminal vessels branching from the abdominal aorta, providing organs like kidneys or liver and so on, additional assumptions have to be stated.

Another method is the up-down approach. Here, the linearised solution is applied on the tree of large vessels to compute its terminal impedances, beginning at the aortic root. Using flow and pressure measurement, the input aortic impedance is determined by measured data and through the trees geometry and its physical parameters the terminal impedances are defined. But it is necessary to have synchronous measurements of flow and pressure waveforms in the aorta, what is not the case usually. Alternatively one of the waveforms may be generated with some measured characteristic parameters.

Chapter 7

Model connection

"Success is the ability to go from one failure to another with no loss of enthusiasm."

Winston Churchill
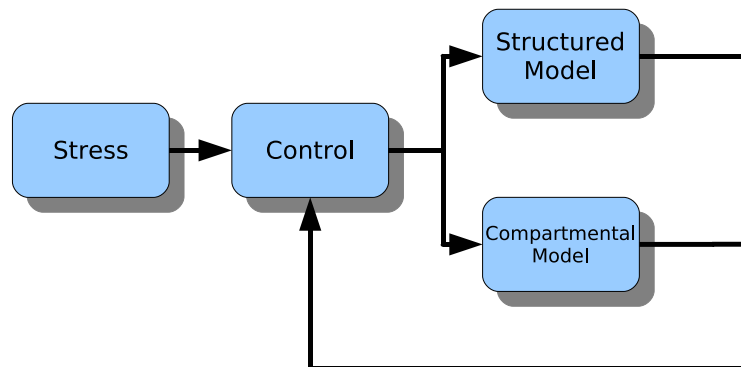
Figure 7.1: *Model connection scheme*

In the previous chapters different approaches for modelling blood flow in human arteries are described, each with its advantages and its disadvantages. Our goal is now to connect the different models to each other to gain the final controlled and identifiable model for the whole cardiovascular system.

On the one hand we have the simplified compartmental model for computing mean values of pressure and flow, considering outer influences as well as the venous part. On the other hand there are the linear and the nonlinear models for the systemic arterial tree, describing blood flow in these arteries, but outer influences, control mechanisms and the venous system are neglected. So the step to connect the different models to each other and make use of its strengths and to compensate its weaknesses is obvious.

The basic strategy for simulating e.g. only the systemic arterial tree is to prescribe pressure and flow waveforms at the systems entry and the parameters on its peripheral segments. Such models are first of all not easy to identify due too much assumptions which had to be and second, there is no dynamic included. Only a steady state of the system can be studied.

Our first approach is now to connect the nonlinear tree model to the compartmental controlled model by computing its system compartment and the nonlinear tree in parallel. The boundary data for the tree models input are determined now by the control, which supplies values for

- mean pressure

- beat volume

- total peripheral resistance

Indeed, the supplied data cannot be used directly because the compartmental model computes mean values only and for the structured tree model pulsatile input data is required.

Furthermore, the synchronisation leads to some serious difficulties because the models are working on different time scales. In the control part one time step is equivalent to one heart beat and after every beat a new value for mean pressure and mean beat volume is computed. But the variables for the nonlinear tree model are discretized in time and the resolution in time is determined by the discretization in space through a stability condition. Furthermore, heart cycles in the nonlinear model are disconnected and its lengths vary in time caused by the change of heart rate due the control
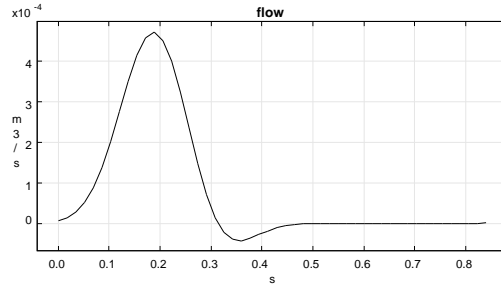
Figure 7.2: *Generated flow wave curve form given heart rate and beat volume with $n = 13$ and $\phi = 0$*

mechanism.

Also when connecting the control mechanism to the linearised tree model dynamical input data have to be generated or extracted from measured data. Stevens et al. [47] published a method for flow wave generation in dependence when a stated heartrate and beatvolume is given. It consists of too parts, one for generating oscillation with pulse frequency, and the second for its wrapping function. After normalising and calibration to measured data a differentiable periodic flow curve is gained in closed form. A resulting flow velocity curve is shown in figure 7.2. The two components of the flow curve are given by

$$Q_1(t, n) = \sin^n(\omega t), \text{ with } n = \text{odd},$$

which defines the wrapping part, and the inner function is defined as

$$Q_2(t, \phi) = \cos(\omega t - \phi)$$

Here, ω is 1.5 times the heart rate and ϕ the phase. The resulting curve is determined by multiplication its two components:

$$Q_3(t, n, \phi) = Q_1(t, n)Q_2(t, \phi)$$

Using this method a suitable aortic flow wave is generated by the controlled compartment model which can be used as terminal condition for the connected nonlinear dynamic model. Due to its generating method the data are smooth enough for the used finite volume algorithm.

Another approach we are discussing is the use of an inverted Windkessel model. The basic idea is the assumption that the left ventricles output work is given through a goodness functional, which minimises energy. Starting from an open system and describing its dynamic behaviour by

$$q(t) = RP \cdot CA \cdot dx + x(t) \tag{7.1}$$

with $q(t)$ aortic flow, $x(t)$ summarised flow through all terminal segments, RP the peripheral resistance and CA the arterial systems compliance, we state a few additional conditions: x(t) is assumed to be periodic if the periodic durations of diastole (t_p) and systole (t_s) are known:

$$x(0) = x_0$$
$$x(t_s) = x_s$$
$$x_s = x_0 \cdot e^{\frac{t_p - t_s}{RA \cdot CA}}$$

Furthermore, flow through the aortic root is set to zero at the end of systole,

$$q(ts) := 0$$

and for a given beat volume (V_S) there holds

$$\int_0^{t_s} q \, dt = V_s \tag{7.2}$$

$$\int_0^{t_s} x \, dt + \int_{t_s}^{t_p} x \, dt = V_s \tag{7.3}$$

which can be seen as conversation of mass. The approximately exponential decrease (validated by measured data) which describes the blood flowing out

from the Windkessel is modeled by

$$x_d(t) = x_s \cdot e^{\frac{t-t_s}{RP \cdot CA}}$$

As discussed in the introduction pressure is mainly determined by the flow and peripheral resistance. Therefore, for the structured models only the prescription of flow in resistance is needed, whereas the definition of flow is easy, one can use the generation method described above. In contrast, the peripheral resistance respectively the total resistance consists of a lot of local parts, distributed on the whole body.

The physical and physiological parameters of vessels change from the proximal to the distal end and can get estimated only at the aortic root, but it is necessary to know the peripheral resistance in every terminal segment of the mapped vascular bed used for the simulation.

Resolving that and distributing the total peripheral resistance, which behaviour is nonlinear, is a difficult task and a good knowledge of the physical parameters of the vessel tree is necessary.

Following, the computation of the two variants of termination models, namely stating complex impedance on termination segments and connecting a Windkessel to each segment are discussed:

Impedance

Knowing the total peripheral resistance and having suitable measured data, using the linearised solution of the Navier-Stokes equations by Womersley leads to some significant advantages. With this analytical solution for describing flow and pressure waveforms in arteries, terminal impedances can be computed and the total peripheral resistance is distributed to the peripheral segments. Doing this we have to compute two different kinds of segments, straight tubes and bifurcations, modelled as one dimensional nodes.

The equations for straight tubes are available in closed form (see chapter 5) and computation is possible from up to down as well as the other way

around, which is not true for bifurcations.
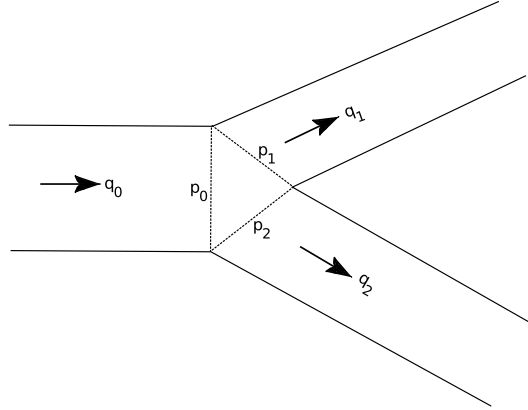
Figure 7.3: *Pressure and flow in a bifurcation*

For computing flow in straight tubes with given input impedance we have to compute mainly the characteristic impedance of the tube and no information of the following vascular bed is needed. This changes if we want to determine impedances or pressure wave forms in bifurcations because the input impedance for every branch has to be computed. If we assume conservation of mass and energy for flow and pressure there holds

1. $q_0 = q_1 + q_2$

2. $p_0 = p_1 = p_2$

and taking into account Ohms law we get for the impedances at any bifurcation

3. $\dfrac{1}{z_0} = \dfrac{1}{z_1} + \dfrac{1}{z_2}$

where z_0 denotes the terminal impedance at the parent vessel and $z1,z2$ the impedances of the daughter vessels. Considering the law of Hagen-Poiseuille,

$$Q = \frac{\pi R^4 (P_1 - P_2)}{8\mu L} \tag{7.4}$$

where Q denotes flow, R the vessels radius, $P_1 - P_2$ the pressure drop, μ the dynamic viscosity and L the length of the segment, we distribute the outflow to the inflow of the daughter vessels by its radii. For the impedance this is possible unless we assume constant pressure wave forms. The stated energy balance which states constant pressure is valid for steady flow and for mean pressure of pulsatile flow, but assuming constant pressure wave forms will avoid nonlinear effects which can be observed on measurements of real blood flow in arteries.

To resolve this we compute impedances of the segments starting from the terminal segments in the beginning of the simulation run. The terminal impedance on each segment is gained by the small vessel replacement model, described in chapter 5. Hence, we are able to compute frequency dependend impedance ratio for the daughter vessels in any bifurcation to their parent vessel. Assuming that the impedance ratio is constant with respect to time and change of total peripheral resistance, the bifurcations are determined now for forward computation during simulation. The assumption of constant impendace ratio implies that the structure of the vessel tree will not change during simulation, which holds for the most applications.

After computing terminal impedances with given total peripheral resistance at the aortic root the parameters for the Windkessels have to be extracted which is done be solving the Windkessel equation 6.4 with the impedance of zero frequency, what defines the total resistance for the considered segment [45]. For the ratio $\frac{R1}{R_T}$ Schaaf [40] suggested 0.2 where the total volume compliance $C_{vol} = 1\text{ml} \cdot \text{mmHg}^{-1}$, published by Burton [6]. After summing up the compliances of each vessels and computing the residual compliance $C_{res} = 1 - C_{total}$ suggested by [40] or [46] and assuming that the residual compliance is distributed among the terminal branches in proportion to their mean flow we gain

$$C_{T_i} = C_{res} \frac{R_{total}}{R_{T_i}} \tag{7.5}$$

where R_{T_i} is the total peripheral resistance and the index T_i denotes the total resistance and compliance at any terminal segment of the vessel tree.

Alternative Method

An alternative approach avoiding the problem or boundary data is to introduce artificial pipes to sum up blood flow in a collection node, similarly to model the venous arteries, but without modelling the network of small vessels and arterioles. This was done by Almeder [2], considering steady flow in human arteries.

This method is seen as being not optimal. One the one hand there are twice more segments to compute, on the other hand the trees structure is not conforming the human physiology anymore due the lack of small arteries. Therefore it can not represent its natural behaviour. Introducing a resistance layer for example would lead to the problem of undetermined parameters again and no benefit is gained.

Chapter 8

Implementation

"A computer once beat me at chess, but it was no match for me at kick boxing."

Emo Philips

The goal of the implementation was to get a framework for experimental blood flow simulation. Due to our modular design and thanks to object oriented programming the different parts can be connected together and substituted by another module quite easily.

The simulation tool is separated into four main parts, implemented in Java and C++. While the graphical user interface (GUI) and the linear models are written in Java, the computational time consuming solver for the nonlinear model part is implemented in C++ and connected to the simulation environment via the Java native interface as a shared library. An overview of the modules is given in table 8.1.

Object oriented programming let us divide the simulation tool into easy supportable modules which are structured as follows.

Graphical user interface	Java
Compartment model solver	Java
Identification tool	Java
Linearised model solver	Java
Nonlinear model solver	C++

Table 8.1: *Module overview of CardioSim*
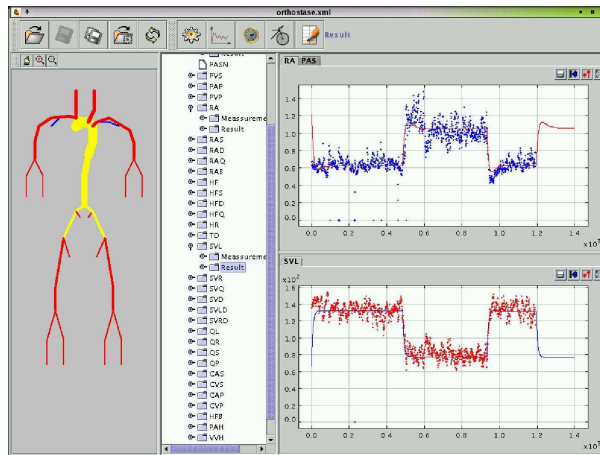
Figure 8.1: *Graphical user interface of the cardiovascular simulation tool*

8.1 Controlled Compartment Model

The solver for the compartmental model consisting of a system of ordinary differential equations of first order is implemented straight forward by Euler's method. Due the smoothness of all data and the equations far away from being stiff, the use of more sophisticated methods is not necessary in our case. Furthermore, the possible numerical error is small compared to the error of the measured data which are taken to verify the gained solution.

In respect to usability of the graphical user interface the solver was implemented as thread and thus its running in the background.

After the simulation run where the time and the initial data can be setted interactively, all variables and parameters can be plotted by drag and drop from the model tree.
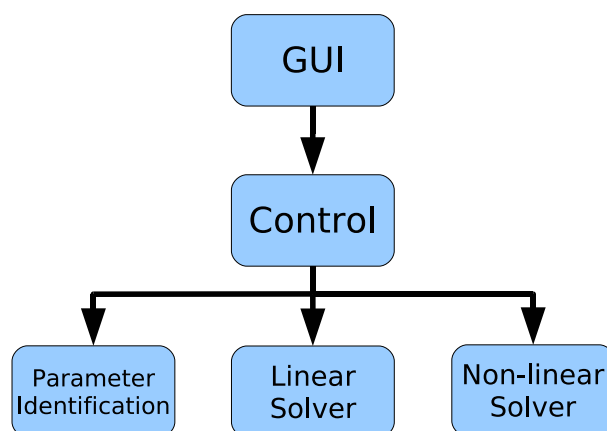
Figure 8.2: *Organisation of the simulation modules*

8.2 Automatic Parameter Identification Tool

Providing also a simple GUI (fig. 8.3) the identification process was implemented following the principle of object oriented programming. The base class `optimizer` contains all necessary setters and getters, whereby the identification process is done by its child classes through heritage. The main method here is the method for calculation the residuum, which is called by the optimizer, the class of the JMSL numeric library providing the optimization algorithm.

After selecting the type of external stress (orthostase or physical stress) the measured values (peripheral resistance, beat volume, heart rate and mean blood pressure) are curve fitted. Then the user has to define the times of state changing, like turning the tilt table test. With this procedure all preprocessing is done and the optimization algorithm tries to identify the necessary parameters. This process is described in a more detailed way in section 4.3.

```
public class OrthostaseOptimizer extends Optimizer
            implements MinConNLP.Function {



  // constructor
```
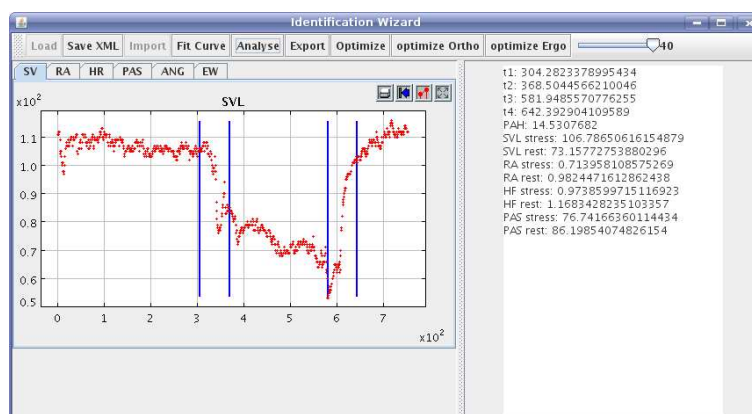
Figure 8.3: The identification wizard with computed parameters

```
public OrthostaseOptimizer(Parameters parms, XMLHandler handler) {


}

// start method
public void run() {
  this.startOptimization();
  }



public void startOptimization() {

  // define the parameter space and constraints
  optiParameters = new double[4];
  this.lowerBounds = new double[]{0.0,0.0,0.0,0.0};

  // get the start values
  optiParameters[0] = ((DParameter) ((DefaultMutableTreeNode)
        currentConfig.getParameterByName("KPAH")).parameter_value;
  optiParameters[1] = ((DParameter) ((DefaultMutableTreeNode)
        currentConfig.getParameterByName("KRA")).parameter_value;
  optiParameters[2] = ((DParameter) ((DefaultMutableTreeNode)
```

```
        currentConfig.getParameterByName("KHFH")).parameter_value;
 optiParameters[3] = ((DParameter) ((DefaultMutableTreeNode)
        currentConfig.getParameterByName("KSVLH")).parameter_value;


// initialize the optimizer
optimization = new MinConNLP(0,0,4);


// set constraints and start values
optimization.setXlowerBound(lowerBounds);
optimization.setGuess(optiParameters);
optimization.setMaxIterations(10);



// start the optimization
try {
    optiParameters = optimization.solve(this);
} catch(Exception ex) {
    ex.printStackTrace();
}


}


// imlementation of the error function, called by the optimizer
public double f(double[] arguments, int iact, boolean[] ierr) {

// get the opjects of the parameters optimized
KPAH = (DParameter) this.currentConfig.
        getParameterByName("KPAH").getUserObject();
KRA = (DParameter) this.currentConfig.
        getParameterByName("KRA").getUserObject();
KHFH = (DParameter) this.currentConfig.
        getParameterByName("KHFH").getUserObject();
KSVLH = (DParameter) this.currentConfig.
```

```java
            getParameterByName("KSVLH").getUserObject();

  // set the paramteres using the optimized values
  KPAH.parameter_value = arguments[0];
  KRA.parameter_value = arguments[1];
  KHFH.parameter_value = arguments[2];
  KSVLH.parameter_value = arguments[3];

  // configure and start the simulator
  cardioSimulator = new CardioControl(this.currentConfig,myBar);
  cardioSettings.simulationTime=this.endTime;
  cardioSimulator.setSimSettings(cardioSettings);
  cardioSimulator.solve();

  // get the considered variables for the minimum function
  newRAl = this.getVariableValue("RA", 90);
  newSVLl = this.getVariableValue("SVL", 90);
  newHFl = this.getVariableVdiscreditedalue("HF", 90);
  newPASl = this.getVariableValue("PAS", 90);

  newSVLs = this.getVariableValue("SVL", 40);
  newHFs = this.getVariableValue("HF", 40);
  newPASs = this.getVariableValue("PAS", 40);*/

  // compute the residuum
  result = Math.sqrt( Math.pow((newRAl -
              parameters.RAStress)/parameters.RAStress,2) +
              Math.pow((newSVLl -
              parameters.SVLStress)/parameters.SVLStress,2) +
              Math.pow((newHFl -
              parameters.HFStress)/parameters.HFStress,2) +
              Math.pow((newPASl -
              parameters.PASStress)/parameters.PASStress,2));
```

```
  // return the residuum
  return result;
}


}
```

8.3 Nonlinear dynamic model

The nonlinear model was implemented by Wibmer [55] in C++ by using a finite volume method for solving the incompressible Navier-Stokes equations in one dimension [11, 12]. It is connected to our model by the java native interface (JNI) which allows the use of shared libraries in java.
Doing this, the needed parameters are given to the library by the native class and the library returns a vector containing the pressure of a specified arterial segment. Furthermore, the library stores all computed data in files which can be read after computation by the GUI.
The java native interface on the java side is implemented as follows whereby under windows to other libraries are loaded separately because there dynamic shared libraries are used. Under linux we are using a static library with all needed files linked together:

```
public class Native {

  public native double[] getPressure( double hf, double ra,...
              double sv,double ampl, int per, int itIndex,...
               int pIndex,int inletType, String inletName,...
               double[] p0, String fname);

    static {
      if ( System.getProperty("os.name").startsWith("Win") ) {
```

```
    System.loadLibrary("xerces-c_2");
    System.loadLibrary("blitz_d");
  }
  System.loadLibrary("anlib");


  }

}
```

Java also provides the C++ header file for native interface. The C++ program must to provide only the function call where the java object types and generic variables are mapped to that of C++.

The C++ source code for our connector is given as follows:

```
#include <jni.h>
/* Header for class hkl_Native */

#ifndef _Included_hkl_Native
#define _Included_hkl_Native
#ifdef __cplusplus
extern "C" {
#endif
/*
 * Class:     hkl_Native
 * Method:    getPressure
 * Signature: (DD)D
 */
JNIEXPORT jdoubleArray  JNICALL Java_hkl_Native_getPressure(...
         JNIEnv *env, jobject obj, jdouble hf, jdouble pr,....
         jdouble svinc,jdouble ampl, jint periods,...
         jint iterationnumber,jint plotdata,jint inlettype,...
         jstring inletname, jdoubleArray jmeanpArray, jstring jxmlFile);
```

```
#ifdef __cplusplus
}
#endif
#endif
```

8.4   Termination value computation

Before every call of the dynamic structured tree model the Windkessel parameters for its terminal segment boundary conditions have to be adopted to the computed total peripheral resistance gained from the control mechanism. First, a root impendace has to be computed from the total peripheral resistance, using a control variable dependent flow curve and a Windkessel. With these data a pressure wave form and further more a complex impendace can be computed.

Using this impedance as initial condition for the linearized model approach from chapter 5, the impedance and hence the Windkessel parameters are gained.

More details are presented in the next chapter.

Chapter 9

Results

"Die Spitze des Berges ist nur ein Umkehrpunkt."

Reinhold Messner

9.1 Linearised model approach

(a) Generated bloodflow

(b) Measured pressure
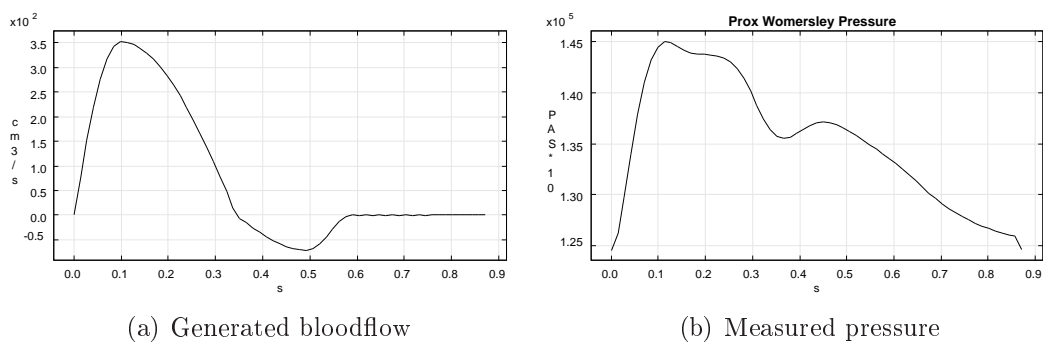
Figure 9.1: Inertial data for the linearised model

Within this first experiment flow and pressure wave forms in the peripheral vessels are computed by prescribing pressure and bloodflow at the aortic root

(a) Pressure   (b) Flow
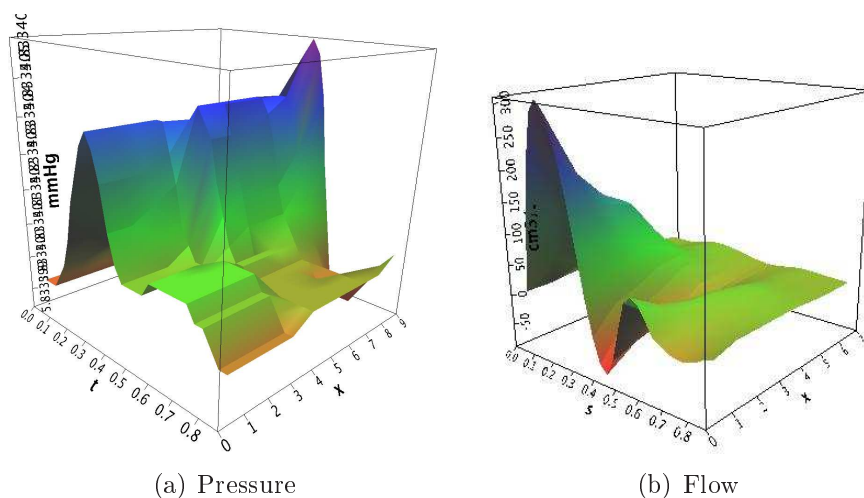
Figure 9.2: *Pressure and flow wave forms and frequency dependent reflection coefficients in different sites in the aorta, a. iliaca and a. femoralis*

(fig. 9.1). Here the volume flow was generated by an ultrasound measured cardiac output and the pressure waveform was taken form the computed waveform by the SphygmoCor software [18, 30]. The model is static and not connected to the control mechanism. Even the model doesn't consider nonlinear viscoelastic effects, it shows that the model covers known phenomenons concerning the pressure wave form very well (fig. 9.5).

The computation is splitted into the following steps:

1. Determination of impedance in the peripheral segments

2. Backward computation of the system and computation of the impedance at the aortic root

3. Calculation of pressure waveforms from impedance and prescribed flow contour

4. Calculation of flow and pressure waveforms along the arterial tree

ad 1

Impedances at several sites are determined by measured flow and pressure curves whereby the phase lag between pressure and flow is not considered. For

(a) Impedance   (b) Reflection coefficient
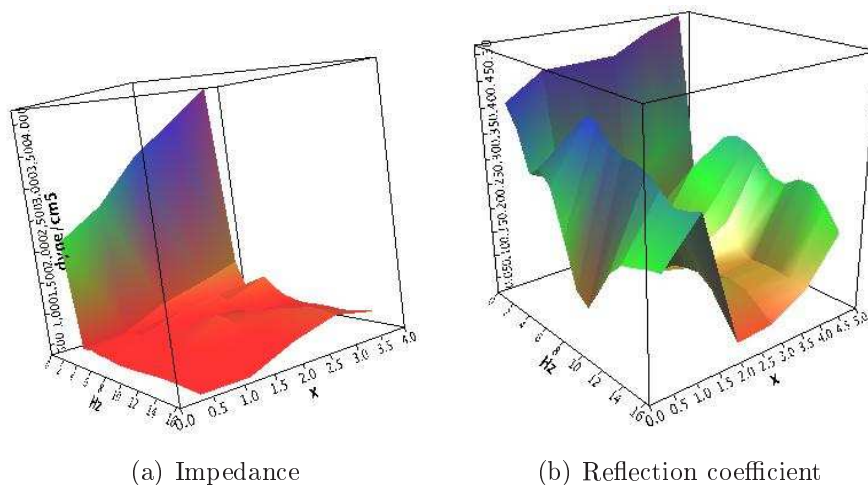
Figure 9.3: *Impedance and reflection coefficients along the aorta*

it, it would be necessary to measure flow and pressure synchronously, what was not possible with our measuring devices. For backward computing of impedances based on measured data another problem occurs: on bifurcations not time-synchronous impedance data would have to be merged (see fig. 9.5 (c) and (d)).

ad 2

With backward computation using the linearised model, the aortic impedance is determined and reflection coefficients are computed for all bifurcations. With help of the reflection coefficients we can compute the reflected and transmitted part of every pressure wave for all arterial segments. Hence, we can consider the influence of the following network of each artery on blood pressure wave forms.

ad 3

The system is completely determined by impedance and pressure *or* flow wave form. One of it must be given as inertial value, where here a flow curve was taken, based on ultrasound measurement. For a measured impedance it would be necessary to determine flow and pressure synchronously in the aortic root, what is only possible with invasive measuring methods.

ad 4
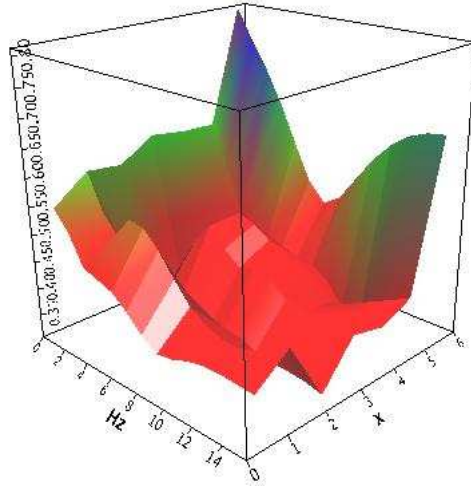
Figure 9.4: *Reflection coefficients along aorta, a. iliac and a. femoralis*

Following to the latter computations pressure and flow wave forms in any arterial segment, beginning with the aortic root, can be computed with the linearised model. The change of pressure and flow wave forms as well as the reflection coefficients at the concerning bifurcations from the aortic root down to the a. femoralis are shown in fig. 9.2.

Remark: Summarising we can say that several important vascular parameters can be determined indirectly with our model and we get realistic results for pressure and flow curves. But it should be mentioned that there is some uncertainty of the results along the aorta, especially in the thorax because the measured data in this area is not of the quality we would need. This part of the arterial system will be considered capsuled.

9.2 Simulation of Pathological Diseases

The following section covers simulation results on influences on the control mechanism. Hence, mainly the compartmental model is considered even due the coupling the whole model might be computed in every experiment like it was done in fig. 9.7 for simulating the tilt table test.

(a) A. brachialis

(b) A. femoralis

(c) A. brachialis

(d) A. femoralis
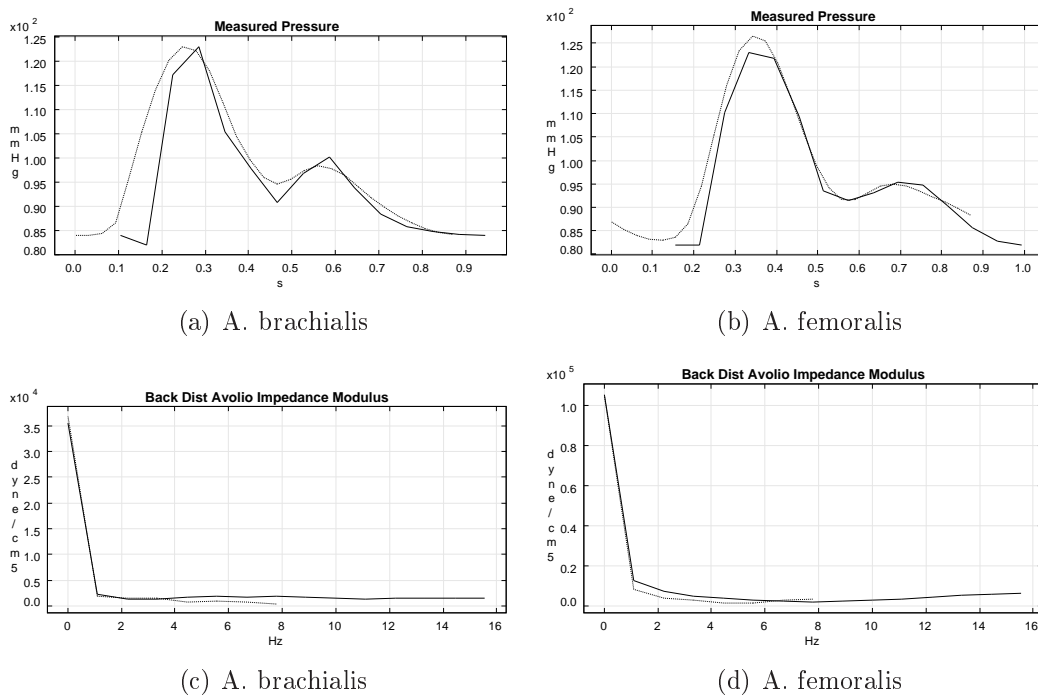
Figure 9.5: *(a) u. (b): Simulated (solid) and measured (dotted) pressure wave forms, (c) and (d): Impedance, from measurement and computed*

9.2.1 Stenosis

Concretions in the arterial vessels cause constrictions, which can be investigated by our model to a certain extent. The influence of these pathological mutations can be considered in a global way. That means that the change of blood pressure downstream the arterial tree can be computed. But, the local flow around the stenosis cannot be considered. This is a task for local 3-dimensional models not covered by our system.

For its simulation we reduce the vessel radius at the considered site within the model of the arterial tree what is increasing the peripheral resistance at his point.
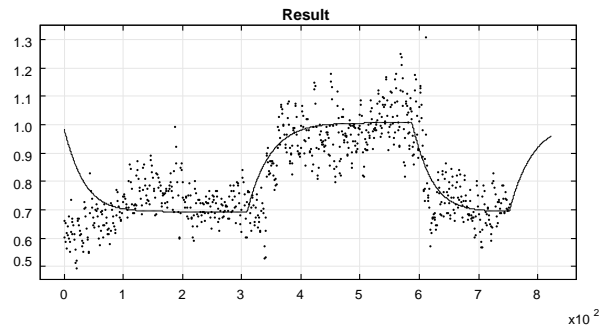
Figure 9.6: *Measurment and simulated (solid line) peripheral resistance during a tilt-table test*
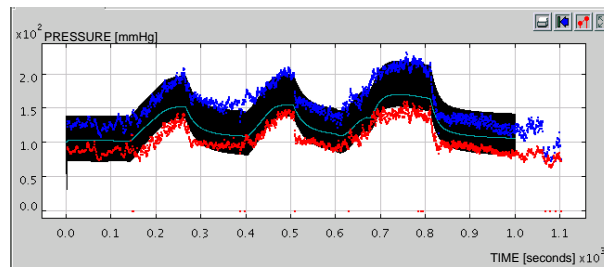
Figure 9.7: *Simulation with the dynamic non-linear structured model during three-phase ergonometry*
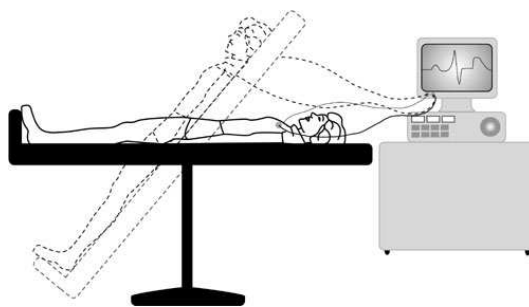
Figure 9.8: *Schematics of a tilt table test*

9.2.2   Tilt Table Test

Using a tilt table a lot of cardiovascular parameters can be identified when measuring blood flow, pressure and ECG. With our model this test can be simulated in an appropriate way. The control mechanism can be adapted to measured data, which defines the inertial data for the structured tree models. Even the transient activity can not be simulated with the linearised model, we can compute pressure and flow in two equilibrium states. That way, the accuracy of our model can be verified by comparison with measured data.

9.2.3   Influences of Drugs on the Cardiovascular System

For treatment of diseases and malfunctions of the cardiovascular system medicists use a wide range of different pharmacological substances. To investigate influences of these drugs on the arterial system qualitatively, we can adapt the concerning model parameters. With our tool pharmacological effects on heart rate, peripheral resistance as well as blood pressure can be simulated. We divide the considered pharmaceuticals into the following groups and give its concerning model parameters.

Some of the most important drugs used in hypertension therapy can be classified as follows:

- Beta Blocker - by adapting the feedback function for the heart rate

- Vasodilatator - by adapting the feedback function for the peripheral resistance

- Diuretikum - by reduction of the blood volume

- ACE Blocker - by adapting the peripheral resistance for the kidneys

- Nitro - reducing the pulmonal pressure

Experiment 1: Nitro

Within this experiment we decreased the pulmonal venous pressure in the compartment model by 20%. Additionally, the peripheral resistance was decreased by 10%, following the oberserved effect of the drug. The results of the simulation run of the four key variables are shown in figure 9.9. Starting from the undisturbed state (red) first the pulmonal venous pressure was lowerd (blue). Here, the peripheral resistance increases because of the control mechanism. Therefor, also the peripheral restistance has to be lowered by a propriate substance (turquoise).

(a) peripheral resistance

(b) stroke volume

(c) mean pulmonal venous blood pressure

(d) mean systemic arterial blood pressure
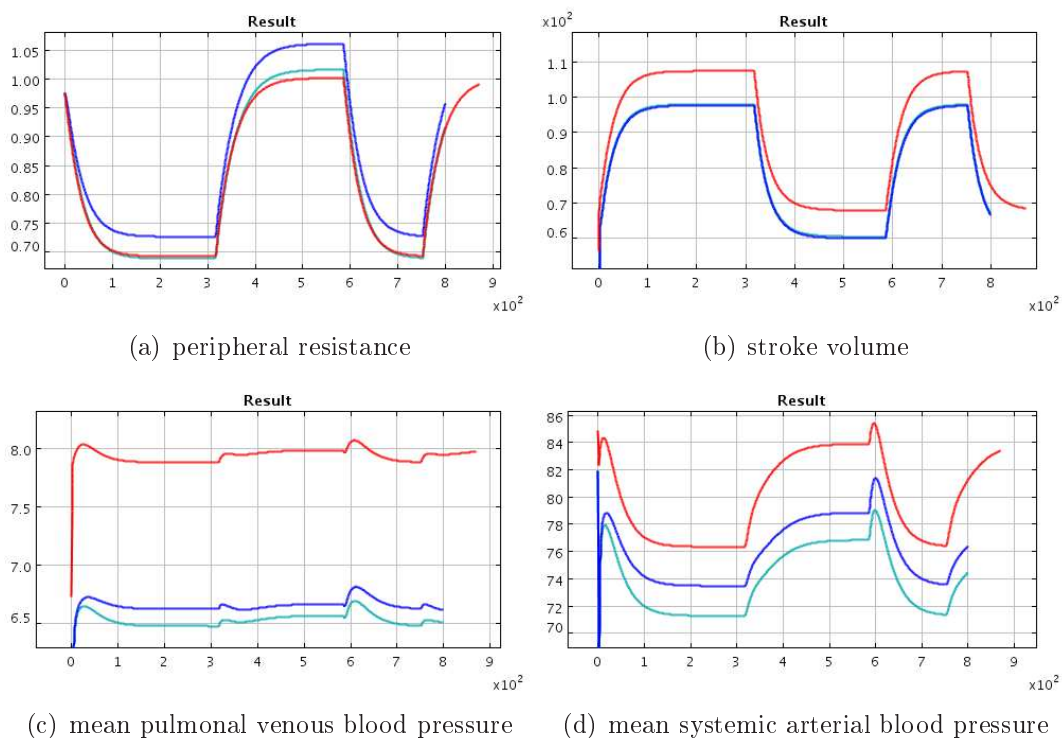
Figure 9.9: *Cardiovascular variables during the tilt table test before (red) and after (blue) decreasing the venous blood pressure and after additional decrease of the peripheral resistance (turquoise)*

Experiment 2: Increase of the stroke volume

Different drugs increase the stroke volume as a side effect. This effect and its consequence on the global haemodynamic was studied by this experiment (figure 9.10).

(a) peripheral resistance

(b) stroke volume

(c) heart rate

(d) mean systemic arterial pressure
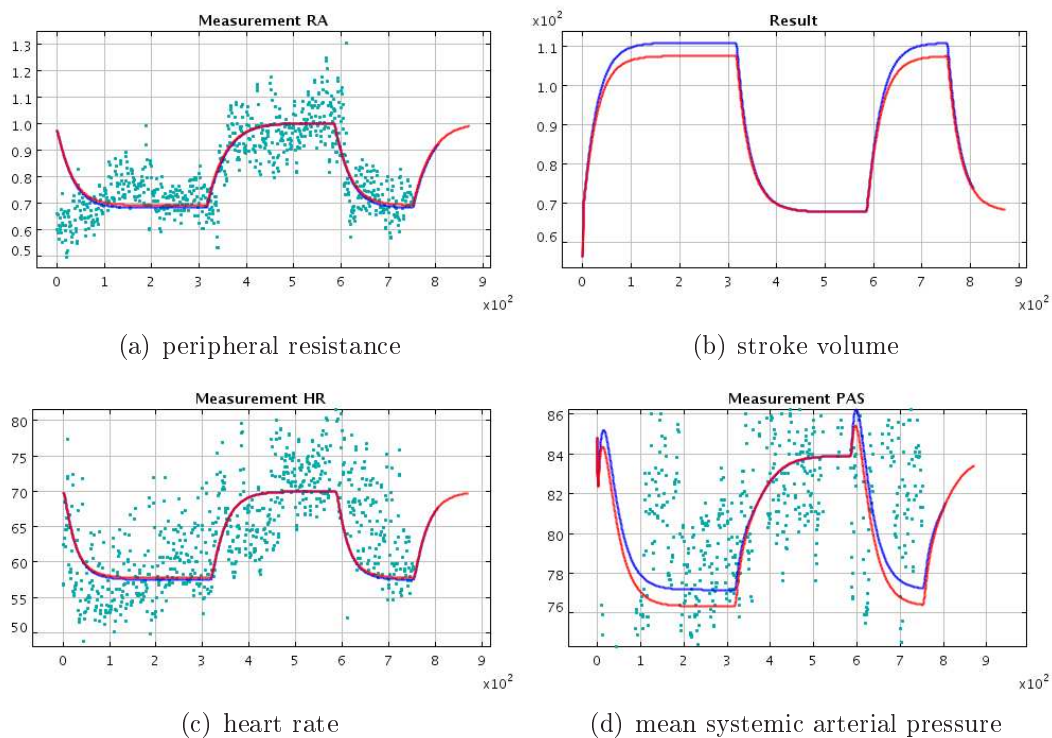
Figure 9.10: *Cardiovascular variables during the tilt table test before (red) and after (blue) lowering the stroke volume*

Experiment 3: β-blocker

In this experiment the usage of so-called β-blockers was simulated (figure 9.11). Doing this, the feedback function of the control mechanism as described in chapter 4 are adopted. The hear rate was lowered by 20% and the peripheral resistance was raised slightly (5%). Due the Frank-Starling mechanism the stroke volume increased by 10% whereby the mean systemic arterial pressure is decreasing by 3%.

(a) peripheral resistance

(b) stroke volume

(c) hear rate

(d) mean systemic arterial pressure
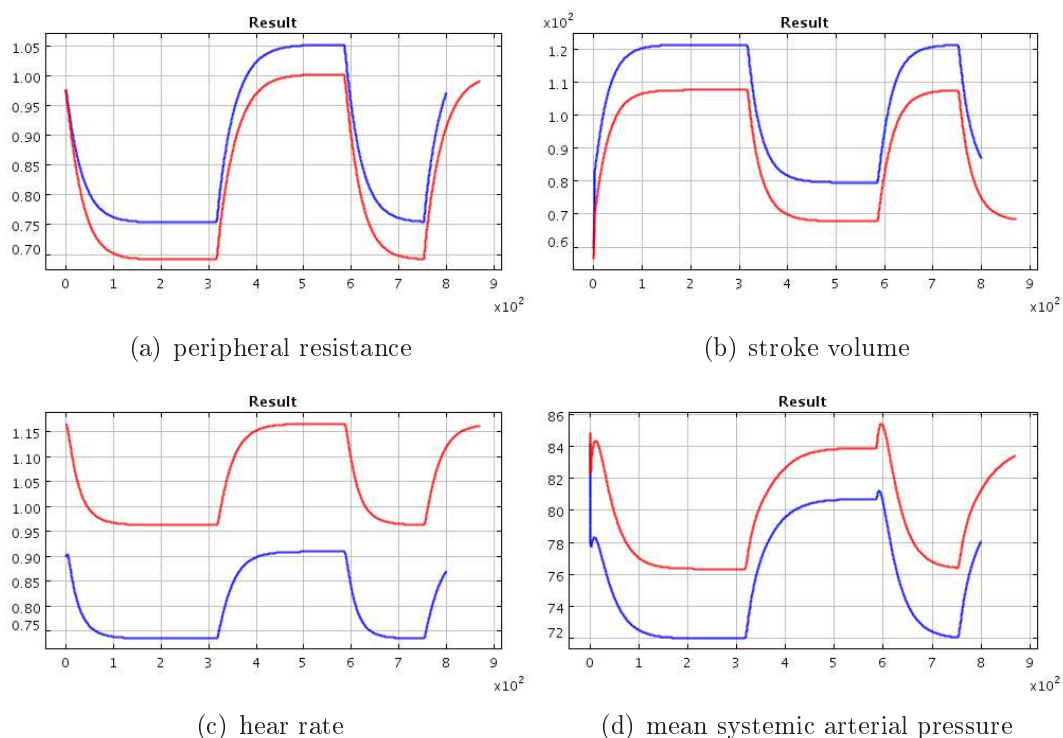
Figure 9.11: *Cardiovascular variables under tilt table test before (rot) and after (blue) β-blocker usage*

9.3 Final coupled model

In the following section results of the whole model connecting all approaches are presented. The simulation run using the control, the linearised approach and the dynamic non-linear model is splitted in steps as follows:

1. Computation of the cardiovascular variables by the controlled compartmental model

2. Generation of the inflow based on the actual magnitudes of beat volume and heartrate

3. Determination of the termination parameters based on the actual peripheral resistance, given by the control mechanism

4. Computation of flow and pressure in arteries by the nonlinear structured tree model

5. Postprocessing of the computed data and continuing with the next cycle
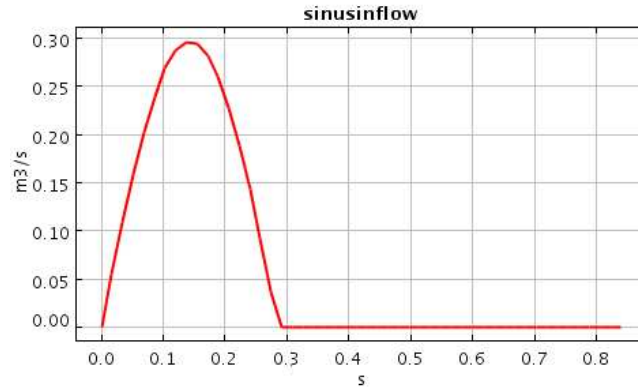
Figure 9.12: *Generated sinus inflow velocity*

From the lumped parameter model, providing the control mechanism, a velocity curve covering the aortic inflow is generated as can be seen in fig. 9.12. Together with the pressure curve which was generated by help of a Windkessel model (fig. 9.13) the impedances of the arterial tree are computed for all vessel segments. Then, at the terminal segments the final total resistances for the terminating Windkessels used by the dynamic model can be determined (tab. 9.2).

With the computed data all boundary values for the dynamic structured tree model are determined. In the shown experiment the data set for the peripheral resistances and capacities are given by table 9.1 using the linearised model.

After computation of steps 1-3 the initial data and boundary values for the dynamical finite volume model are known and the simulation run is started. The computed data are plotted for three different values of x for each segement ($x = 0$, $x = l/2$, and $x = l$ with l denoting the length of the vessel).

In figure 9.14 the pressure and flow curves of the simulation run compared with measured data are shown. The pressure wave form was measured by

tonometry where the systolic and diastolic pressure was adapted because it can not be measured by the used technique. It is taken using a separate common measurement device. The flow measurement was done by doppler ultrasonic measurement. It shows that the computed wave forms match the measured ones very well (fig. 9.16 and fig. 9.17).

Pressure and flow forms on different sites along the arterial tree are plotted in picture 9.14. The observed effects, namely increase of systolic pressure and higher steepness of the pressure waveform can be observed. Also the change of the flow waveform matches the measured flows as well as curves which can be found in literature.
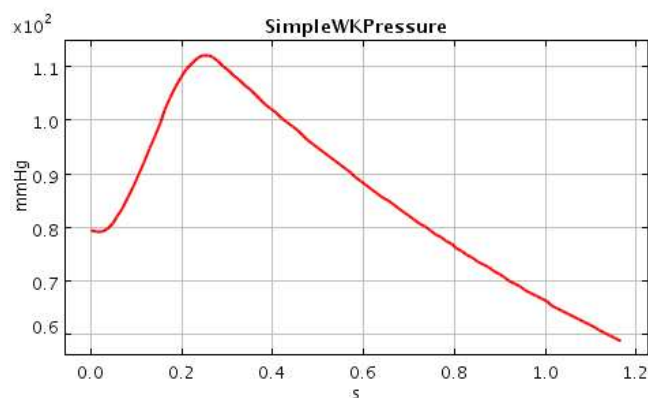
Figure 9.13: *Windkessel generated pressure at the aortic root*
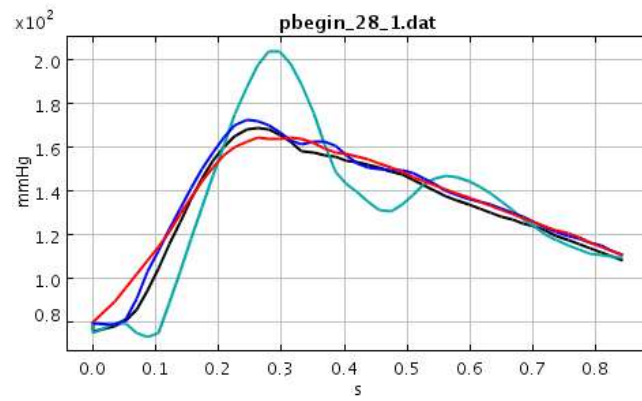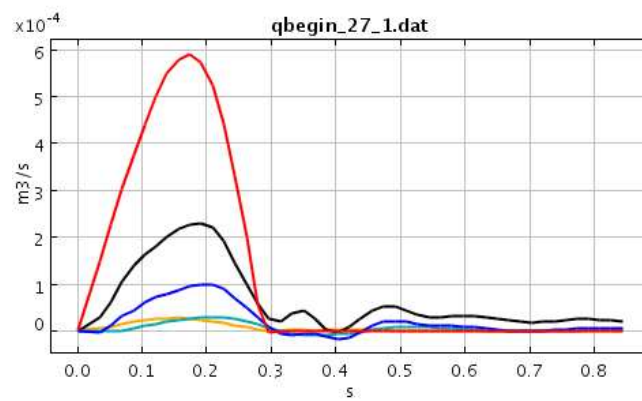
(a) pressure

(b) flow

Figure 9.14: *Pressure and flow wave forms along the vascular tree (aortic root, abdominal aorta, brachial artery and femoral artery*
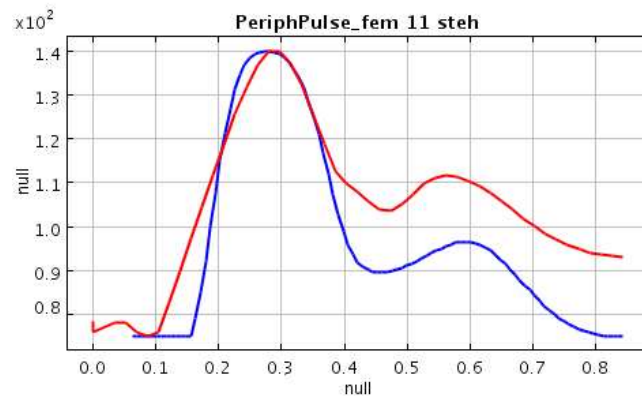
(a) pressure
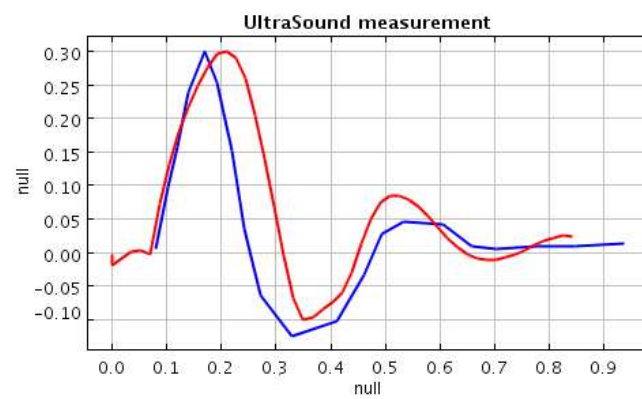
(b) flow

Figure 9.15: *Pressure and flow wave forms at the femoral artery (red) , compared with measurement (blue)*
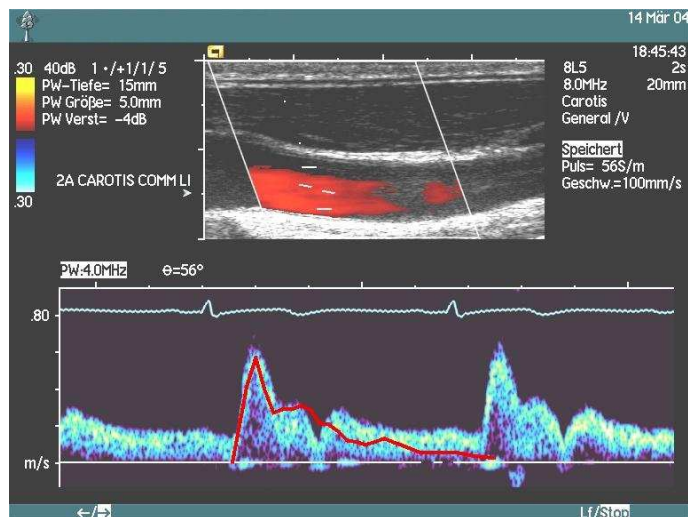
Figure 9.16: *Comparison of computed flow velocity with ultrasound measurement in the carotid artery*
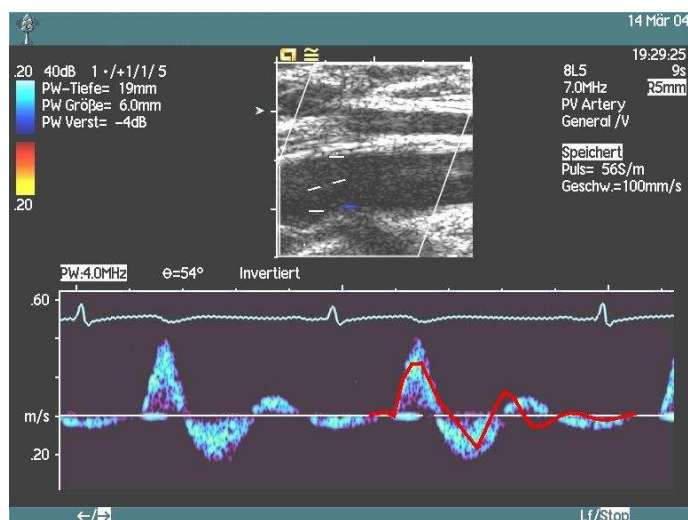
Figure 9.17: *Comparison of computed flow velocity with ultrasound measurement in the femoral artery*

Segment	Name	Length (m)	Proximal Radius (m)	Distal Radius (m)	Wave speed (m/s)
1	Ascending A	0.02	0.0147	0.0147	4.3
2	Ascending B	0.02	0.0144	0.0144	4.3
3	Arc A	0.02	0.0112	0.0112	4.3
4	Arc B	0.039	0.0107	0.0107	4.3
5	Thoracic A	0.052	0.0099	0.0099	4.3
6	Thoracic B	0.104	0.00675	0.00645	4.3
7	Common Iliac R	0.058	0.00368	0.0035	5.0
8	External Iliac R	0.144	0.0032	0.0027	6.0
9	Internal Iliac R	0.05	0.0020	0.0020	6.0
10	Deep Femoralis R	0.126	0.00255	0.00186	9.0
11	Femoralis R	0.443	0.00259	0.0019	7.3
12	Common Iliac L	0.058	0.00368	0.00365	5.0
13	Internal Iliac L	0.05	0.0020	0.0020	6.0
14	External Iliac L	0.144	0.0032	0.0027	6.0
15	Femoralis L	0.443	0.00259	0.0019	7.3
16	Deep Femoralis L	0.126	0.00255	0.00186	9.0
17	Subclavian	0.034	0.00423	0.00423	4.5
18	C Carotid L	0.208	0.0037	0.0037	13.055
19	Brachiocephalic	0.034	0.0060	0.0060	4.5
20	C Carotid R	0.177	0.0037	0.0037	13.055
21	Subclavian	0.034	0.00423	0.00423	4.5
22	Vertebral R	0.148	0.00188	0.00188	7.0
23	Brachialis R	0.422	0.00403	0.00236	3.3
24	Radialis R	0.235	0.00174	0.00142	8.0
25	Ulnar I R	0.067	0.00215	0.00215	6.0
26	Vertebral L	0.148	0.00188	0.00183	7.0
27	Brachialis L	0.422	0.00403	0.00236	7.0
28	Radialis L	0.235	0.00174	0.00142	8.0
29	Ulnar I L	0.067	0.00215	0.00215	6.0

Segment	Name	Length (m)	Proximal Radius (m)	Distal Radius (m)	Wave speed (m/s)
30	Tibial Ant R	0.343	0.0013	0.0013	10.0
31	Tibial Post R	0.321	0.00247	0.00141	10.0
32	Tibial Post L	0.321	0.00247	0.00141	10.0
33	Tibial Ant L	0.343	0.0013	0.0013	7.6
34	Intercostals	0.08	0.0020	0.0015	3.6
35	Celiac Axis	0.04	0.0039	0.0039	5.4
36	Hepatic A	0.066	0.0022	0.0022	4.7
37	Hepatic B	0.03	0.0018	0.0018	4.5
38	Splenic	0.063	0.00275	0.00275	4.5
39	Gastric	0.071	0.0018	0.0018	4.9
40	Abdominal A	0.053	0.0061	0.0061	4.3
41	Superminor Mesenteric	0.059	0.00434	0.00434	4.1
42	Abdominal B	0.02	0.0060	0.0060	4.3
43	Renal	0.032	0.0026	0.0026	4.5
44	Abdominal C	0.02	0.0059	0.0059	4.8
45	Renal	0.032	0.0026	0.0026	4.3
46	Abdominal D	0.106	0.0058	0.00548	4.3
47	Inferior Mesenteric	0.05	0.0016	0.0016	5.0
48	Abdominal E	0.02	0.0052	0.0052	4.3
49	Carotid External R	0.177	0.00177	8.3E-4	10.0
50	Carotid Internal R	0.177	0.00177	8.3E-4	10.0
51	Carotid Internal L	0.177	0.00177	8.3E-4	10.0
52	Carotid External L	0.177	0.00177	8.3E-4	10.0
53	Ulnar II L	0.171	0.00203	0.00183	8.0
54	Interosseous L	0.079	9.1E-4	9.1E-4	8.0
55	Ulnar II R	0.171	0.00203	0.00183	8.0
56	Interosseous R	0.079	9.1E-4	9.1E-4	8.0

Table 9.1: Physiological data for the arterial tree

Segment	Node	Total resistance	Total compliance
		N s m−5	N5 m-1
9	9	7.936E9	2.3E-11
10	11	4.77E9	3.9E-11
13	14	7.936E9	2.3E-11
16	17	4.77E9	3.9E-11
22	27	6.01E9	3.0955E-11
24	29	5.28E9	3.5235E-11
26	23	6.01E9	3.0955E-11
28	21	5.28E9	3.5235E-11
30	31	5.59E9	3.3281E-11
31	32	4.77E9	3.9003E-11
32	33	4.77E9	3.9003E-11
33	34	5.59E9	3.3281E-11
34	36	1.39E9	1.3384E-10
36	39	3.63E9	5.1251E-11
38	41	2.32E9	8.0E-11
39	42	5.41E9	3.4389E-11
41	44	9.3E8	2.0005E-10
43	45	1.13E9	1.6464E-10
45	47	1.13E9	1.6464E-10
47	49	6.88E9	2.7041E-11
49	51	1.39E10	1.3384E-11
50	52	1.39E10	1.3384E-11
51	53	1.39E10	1.3384E-11
52	54	1.39E10	1.3384E-11
53	20	5.28E9	3.5235E-11
54	56	8.43E10	2.2068E-12
55	30	5.28E9	3.5235E-12
56	58	8.43E10	2.2068E-12

Table 9.2: *Termination segment impedance data*

Chapter 10

Conclusion and Future Prospects

"My advice to you is get married: if you find a good wife you'll be happy; if not, you'll become a philosopher."

Socrates

This thesis covers three different approaches for simulation of blood flow in human arteries, which are connected to each other to get an one-dimensional controlled identifiable dynamic model of the cardiovascular system. It shows the advantages and disadvantages of each approach and also other, not considered approaches are mentioned and the differences are discussed.

Although a lot of accurate models can be found in the literature, most of them are verified against one dataset, very often against the same one. Furthermore, usually the 1-dimensional dynamic models based on the Navier-Stokes equations are static in the sense of initial- and boundary values.

Our model adapts the boundary and initial values for the aortic root (inflow) as well as for the termination segments (outflow) before each heart cycle. Together with the identification procedure for the controlled compartment model it can be fully identified concerning physiological parameters. For the identification algorithm only measurements from non-invasive methods are

used. Physical parameters like artery lengths and diameters are much more difficult and expensive to measure. They could be determined within our possibilities only partly through Doppler ultrasonic technique. Missing data were taken either from the literature or interpolated by given data.

Summarizing, the identification of the model parameters can be seen as the most difficult and time consuming task. On the one hand it is difficult to get measured data of good quality, on the other hand the main part of the evaluation of measured data must be done by hand, even some tools for its automation were developed during the work on this project. For practical use of such a simulation tool described in this thesis it is important that the identification process can be done by data from non-invasive measurement only. Its disadvantages, e.g. that flow and pressure are usually not synchronous was explained in the last section.

Even our model covers already many physiological phenomenons, there is still place for further improvements. At first, the non-linear finite volume implementation was figured out to be unstable concerning realistic initial data. As consequence it should be revised and might be replaced by a finite element implementation.

Furthermore, our model does not cover a model of the heart what can be also a future task, whereby the question of the heart models parameter identification has to be solved also. For our simulation runs the measured output of the left ventricle was used instead. For it, no parameter has to be determined.

Appendix A

Formulas

If we write $y := \frac{r}{R}$ the velocity yields to

$$w = +\frac{A}{\rho}\frac{1}{in}\left\{1 - \frac{J_0\left(\alpha y i^{\frac{3}{2}}\right)}{J_0\left(\alpha i^{\frac{3}{2}}\right)}\right\}e^{int} \tag{A.1}$$

This is still in complex form. For the real part of the flow in equation A.1 we take the corresponding part of the pressure gradient Ae^{int}. First, we write the Besselfunctions in the Euler notation for complex numbers:

$$J_0(\alpha y i^{\frac{3}{2}}) = M_0(y)e^{i\theta_0(y)}$$
$$J_0(\alpha i^{\frac{3}{2}}) = M_0 e^{i\theta_0}$$

Divergence theorem:

$$\int_S \boldsymbol{F} \cdot \boldsymbol{n}\,\mathrm{d}S = \int_V \nabla \cdot \boldsymbol{F}\mathrm{d}V \tag{A.2}$$

and one of its identities is

$$\int_S \Phi\boldsymbol{n} = \int_V \nabla\Phi\mathrm{d}V \tag{A.3}$$

Appendix B

Measured Data

Here one dataset obtained from a set of ultrasound measurements is given.

We determined aortic diameter, flow velocity, pulse wave propagation velocity and the heart rate. In the following tables the flow velocity curves are not given, they are generated from images within the simulation environment after the calibration was done manually.

All our measured data are documented and archived on a DVD and the given file names are references to it, but for copyright reasons the DVD could not be attached to this work. If the reader has further questions or wants to verify the measured data he should not hesitate to contact the author or somebody else from his working group.

All given parameters were obtained be analysing bitmap images with the open source software DICOMWORKS.

Person data	
Patienten #	
Age	24
Weight	56kg
Height	175cm
Sex	m
Systole	93
Diastole	64
	liegend
# of series	1
Date of measurement	38060
Hypersonic device:	Aceson

Table B.1: *Person data*

Measurement: DIAMETER				
	Picture # in series	Picture # in print	SYSTOLE (cm)	DIASTOLE (cm)
Aortic root	9	A1		1.98
	10	A2		2.14
	11	A3		2.13
	12	A4		2.14
Carotis Communis left	22	A5	0.66, 0.66, 0.66	0.59, 0.58, 0.58
Carotis Communis right	28	A6	0.57, 0.58, 0.57	0.49, 0.48, 0.49
	29	A7	0.58, 0.57	0.50, 0.49
Radialis right	78	A8		0.222, 0.232, 0.236, 0.237, 0.236
Radialis left	107	A9		0.225, 0.242, 0.218, 0.218, 0.218
Abdominlalis aorta (bifurcation)	130	A10	1.37, 1.38, 1.38	1.29, 1.29, 1.30
	141	A11		1.405, 1.373, 1.359, 1.350, 1.381
Iliac Externa right	153	A12		0.817, 0.824, 0.831
Arteria Pop right	161	A13	0.56, 0.56, 0.57	0.49, 0.5, 0.5
Arteria Tibialis right	186	A14		0.194, 0.214, 0.218, 0.198

Table B.2: *Measurement of the aortic diameter from ultrasound images*

Measurement: LENGTH OF PERIOD				
	Picture # in series	Picture # in print	TIME [s]	PULSE [beats/ minute]
Carotis Communis left	13	A15	1.11, 1.12	56
	15	A16	1.07	56
Carotis Communis right	36	A17	1.11	49
	38	A18	1.03	58
Radialis right	76	A19	1.12, 1.04	54
Radialis left	103	A20	0.98	50
	105	A21	1.12	53
Abdominlalis Aorta (bifurcation)	132	A22	1.13	54
	143	A23	1.16	52
Iliac Externa right	146	A24	1.1	56
A pop right	165	A25	1.08	56
	173	A26	1.03	56
A tibialis right	184	A27	1.1	55

Table B.3: *Measurement of period length*

Measurement: SIGNAL RUNNING TIME			
	Picture # in series	Picture # in print	TIME [s]
Aortenwurzel	5	A28	0.07
Cartois Communis left	14	A29	0.09, 0.08, 0.09,0.1
Carotis Communis right	35	A30	0.08, 0.08
Radialis right	73	A31	0.18, 0.18
Radialis links	93	A32	0.18, 0.18
Distal Aorta (bifurcation)	136	A33	0.16, 0.16
Iliac right	147	A34	0.17, 0.18
Arteria Pop right	165	A35	0.23, 0.22
Arteria Tibialis right	183	A36	0.26, 0.27
	184	A37	0.24, 0.26, 0.27

Table B.4: *Measurement of the pressure amplitude velocity*

Bibliography

[1] D. J. Acheson. *Elementary fluid dynamics*. Oxford Applied Mathematics and Computer Science Series. Oxford University Press, Oxford, New York, 1990.

[2] Christian Roland Almeder. *Hydrodynamic modelling and simulation of the human arterial blood flow*. PhD thesis, Vienna University of Technology, Austria, 1999.

[3] A. P. Avolio. Multi-branched model of the human arterial system. *Med. & Biol. Eng. & Comput.*, 18:709–718, 1980.

[4] D. H. Bergel. The dynamic elastic properties of the arterial wall. *J. Physiology*, 156:458, 1961.

[5] R. Botnar, G. Rappitsch, M. B. Scheidegger, D. Liepsch, K. Perktold, and P. Boesiger. Haemodynamics in the carotid artery bifurcation: a comparison between numerical simulations and in vitro mri measurements. *J. Biomechancis*, 33:137–144, 2000.

[6] A. C. Burton. Physiology and biophysics of the circulation. *Yearbook Medical Publishers*, 1965.

[7] L. Formaggia, J. F. Gerbeau, F. Nobile, and A. Quarteroni. On the coupling of 3d and 1d navier–stokes equations for flow problems in compliant vessels. *Comput. Meth. Appl. Mech. Eng.*, 191(6-7):561–582, 2001.

[8] L. Formaggia, D. Lamponi, and A. Quarteroni. One dimensional models for blood flow in arteries. *J. Eng. Math.*, 47(3-4):251–276, 2003.

[9] O. Frank. Die Grundform des arteriellen Pulses. *Zeitschrift für Biologie*, 37:483, 1899.

[10] O. Frank. Der Puls in den Arterien. *Zeitschrift für Biologie*, 45:441–553, 1905.

[11] G. P. Galdi, J. G. Heywood, and R. Rannacher, editors. *Contributions to current challenges in mathematical fluid mechanics*. Advances in mathematical fluid dynamics. Birkhäuser, Basel, 2004.

[12] E. Godlewski and P. A. Raviart, editors. *Numerical approximation of hyperbolic systems of conservation laws*, volume 118 of *Applied mathematical sciences*. Springer, New York, 1996.

[13] S. Hales. *Statical essays: containing haemostaticks, or an account of some hydraulick and hydrostatical experiments made on the blood and blood vessels of animals.* Innys & Manby, London, 1733.

[14] V. Hardung. Über eine Methode zur Messung der dynamischen Elastizität und Viskosität kautschukähnlicher Körper, insbesondere von Blutgefäßen und anderen elastischen Gewebeteilen. *Helvetica Physiologica Acta*, 10:482–498, 1952.

[15] V. Hardung. Vergleichende Messungen der dynamischen Elastizität und Viskosität von Blutgefäßen, Kautschuk und synthetischen Elastomeren. *Helvetica Physiologica Acta*, 11:194–211, 1953.

[16] V. Hardung. Propagation of pulse waves in viscoelastic tubing. In W. F. Hamilton and P. Dow, editors, *American Physiological Society handbook of physiology*, volume 1, page 107. Washington DC, 1962.

[17] E. P. W. Helps and D. A. McDonald. Systolic backflow in the dog femoral artery. *J. Physiology*, 122:73, 1953.

[18] R. Klocke, J. R. Cockcroft, G. J. Taylor, I. R. Hall, and D. R. Blake. Arterial stiffness and central blood pressure, as determined by pulse wave analysis, in rheumatoid arthritis. *Ann Rheum Dis*, 62:414–418, 2003.

[19] J. Kropf. Dynamische Herzkreislaufsimulation unter Berücksichtigung verteilter Parameter. Master's thesis, Technical University of Vienna, Austria, 2003.

[20] A. Laganà, G. Dubini, F. Migliavacca, R. Pietrabissa, G. Pennati, G. Veneziani, and A. Quarteroni. Multiscale modelling as a tool to prescribe realistic boundary conditions for the study of surgical procedures. *Rheology*, 39(3-4):359 − 364, 2002.

[21] J. K. Li, J. Melbin, R. A. Riffle, and A. Noordergraaf. Pulse wave propagation. *Circ res*, 49:442–452, 1981.

[22] J. Lighthill. *Waves in fluids*. Cambridge University Press, 1978.

[23] D. A. McDonald. The velocity of blood flow in rabbit aorta studied with high-speed cinematography. *J.Physiology*, 118:328–339, 1952.

[24] D. A. McDonald. The relation of pulsatile pressure to flow in arteries. *J. Physiology*, 127:533–552, 1955.

[25] J. Melbin and A. Noordergraaf. General solution for flow and stress phenomena in elastic vessels (Navier-Stokes). *Bull Bath Biol*, 44:29–42, 1982.

[26] C. J. Mills, I. T. Gabe, and J. H. Gault. Pressure-flow relationships and vascular impedance in man. *Cardiovascular Research*, 4:405–417, 1970.

[27] W. R. Milnor. *Hemodynamics*. Williams & Wilkins, 1989.

[28] A. I. Moens. *Die Pulskurve*. Leiden, 1878.

[29] Dieter Möller, Dobrivoje Popović, and Georg Thiele. *Modeling, simulation and parameterestimation of the human cardiovascular system*, volume 4 of *Advances in Control Systems and Signal Processing*. Vieweg, 1983.

[30] W. W. Nichols. Clinical measurement of arterial stiffness obtained from noninvasive pressure waveforms. *Am J Hypertens*, 18:3S–10S, 2005.

[31] Wilmer W. Nichols and Michael F. O'Rourcke. *McDonald's blood flow in arteries*. Arnold, 1998.

[32] M. S. Olufsen. Structured tree outflow condition for blood flow in larger systemic arteries. *Am J Physiol, Heart and Circ Physiol*, 276:H257–H268, 1999.

[33] M. S. Olufsen, C. S. Peskin, W. Y. Kim, Pedersen E. M., A. Nadim, and Larsen J. Numerical simulation and experimental validation of blood flow in arteries with structured-tree outflow conditions. *Annals of Biomedical Engineering*, 28:1281–1299, 2000.

[34] T. Pedley. *The fluid mechanics of large blood vessels*. Cambridge University Press, Cambridge, 1980.

[35] K. Perktold and G. Rappitsch. Computer simulation of the local blood flow and vessel mechancis in a compliant carotid artery bifurcation model. *J. Biomechancis*, 28(7):845–856, 1995.

[36] L. H. Peterson, R.E. Jensen, and J. Parnell. Mechanical properties of arteries in vivo. *Circulation Research*, 8:622–639, 1960.

[37] L. Prandtl, K. Oswatitsch, and K. Wieghardt. *Führer durch die Strömungslehre*. Vieweg, 9 edition, 1942.

[38] A. Quarteroni and L. Formaggia. Mathematical modelling and numerical simulation of the cardiovascular system. In P. G. Ciarlet, editor, *Special volume: computational models for the human body*, volume 12 of *Handbook of Numerical Analysis*. Elsevier, Amsterdam, 2004.

[39] J. K. Raines, M. Y. Jaffrin, and A.H. Shapiro. A computer simulation of arterial dynamics in human legs. *J. Biomech.*, 7:77–91, 1974.

[40] B. W. Schaaf and P. H. Abbrecht. Digital computer simulation of human systemic arterial pulse transmission: a non-linear model. *J. Biomechanics*, 5:345–364, 1972.

[41] S. J. Sherwin, L. Formaggia, J. Peiró, and V. Franke. Computational modelling of 1d blood flow with variable mechanical properties and its application to the simulation of wave propagation in the human arterial system. *Int. J. Numer. Meth. Fluids*, 43:673–700, 2003.

[42] H. A. Snellen. *E. J. Marey and cardiology*. Kooyker, Rotterdam, 1980.

[43] P. Spellucci. A new technique for inconsistent problems in the sqp method. *Math. Meth. of Oper. Res.*, 47:355–500, 1998.

[44] P. Spellucci. An sqp method for general nonlinear programs using only equality constrained subproblems. *Math. Prog.*, 82:413–448, 1998.

[45] N. Stergiopulos, B. E. Westerhof, and N. Westerhof. Physical basis of pressure transfer from periphery to aorta: a model-based study. *AJP - Heart*, 274:1386–1392, 1998.

[46] N. Stergiopulos, D. F. Young, and T. R. Rogge. Computer simulation for arterial flow with applications to arterial and aortic stenoses. *J. Biomechanics*, 25(12):1477–1488, 1992.

[47] S. A. Stevens, W. D. Lakin, and W. Goetz. A differentiable, periodic function for pulsatile cardiac output based on heart rate and stroke volume. *Mathematical Biosciences*, 182:201–211, 2003.

[48] Y. Stickler. Dynamisches Modell des Herzkreislaufs mit Regelung. Master's thesis, Technical University of Vienna, Austria, 2002.

[49] M. G. Taylor. The experimental determination of the propagation of fluid oscillations in a tube with a viscoelastic wall; together with an analysis of the characteristics required in an electrical analogue. *Phys. Med. Biol.*, 4:63, 1959.

[50] I. E. Vignon and C. A. Taylor. Outflow boundary conditions for one-dimensional finite element modeling of blood flow and pressure waves in arteries. *Wave Motion*, 39:361–374, 2004.

[51] J. Wan, B. Steele, S. A. Spicer, S. Strohband, G. R. Feijóo, T. J. R. Hughes, and C. A. Taylor. A one-dimensional finite element method for simulation-based medical planning for cardiovascular disease. *Comput. Meth. Biomech. Biomed. Eng.*, 5:195–206, 2002.

[52] J. Wang, A. B. O'Brien, N. G. Shrive, K. H. Parker, and J.V. Tyberg. Time-domain representation of ventricular-arterial coupling as a windkessel and wave system. *AJP - Heart*, 284:1358–1368, 2003.

[53] J. J. Wang and K. H. Parker. Wave propagation in a model of the arterial circulation. *J. Biomechancis*, 37:457–470, 2004.

[54] N. Westerhof and A. Noordergraf. Arterial viscoelacticity: a generalised model. *J. Biomechanics*, 3:357, 1970.

[55] M. Wibmer. *One-dimensional simulation of arterial blood flow with applications*. PhD thesis, Vienna University of Technology, Austria, 2004.

[56] J. R. Womersley. Method for the calculation of velocity, rate of flow and viscous drag in arteries when the pressure gradient is known. *J. Physiology*, 127:553–563, 1955.

[57] J. R. Womersley. The mathematical analysis of the arterial circulation in a state of oscillatory motion. Technical Report WADC-TR56-614, Wright Air Development Centre, 1957.

[58] J. R. Womersley. Oscillatory flow in arteries. ii: the reflection of the pulse wave at junctions and rigid inserts in the arterial system. *Phys Med Biol.*, 2(4):313–323, 1958.

List of Figures

Curriculum Vitae

Johannes Kropf

Address: Brachelligasse 28 Haus 7, A-1220 Wien

Telephone: +43-699-815-118-61

E-mail: johannes@kropf.at

Homepage: http://johannes.kropf.at

Date of Birth: 17.08.1976, in Fürstenfeld, Austria

Nationality: Austrian

Marital status: married to Tetiana

Degree: Diplom-Ingenieur (Dipl.-Ing.) - comparable with Master of Science

Educational Record

since 07/2006	Research assistant at the institute for Analysis and Scientific Computing
09/2003 -05/2006	Research assistant and Ph.D. student and the Institute for Analysis and Scientific in collaboration with the Austrian research centres Seibersdorf
	recent research project: "Modelling and Simulation of the Human Cardiovascular System"
06/2003	Diploma in technical Mathematics (with distinction)

09/1996 - 06/2003	Studies of technical mathematics at Graz University of Technology and Vienna University of Technology, Austria
	Focus: applied mathematics, modelling and simulation, numerical mathematics, computer sciences
05/1995	Final highschool degree (Matura), BG\BRG Fürstenfeld
09/1986 - 05/1995	Primary and secondary school

Work Experience

since 09/2003	Research assistant at the Vienna University of Technology in the fields of modelling and simulation and applied mathematics
since 09/2000	System administrator at the Institute for Analysis and Scientific Computing, Vienna University of Technology
01/2000 - 01/2001	Running my own company: Internet-services and IT consulting

Knowledge of Languages	German: native
	English: ready for negotiation
	French: ready for conversation
	Russian: basics, studying in progress
Further Knowledge	Highly sophisticated software developer
	Highly sophisticated in IT
Alternative Service	Done 10/1995 - 09/1996 at Lebenshilfe Feldbach, Austria

Hobbies   Rock Climbing - let me see that a lot what seems to
                     be impossible becomes possible with a strong mind
                     Orienteering - let me train to make right decisions
                     quickly and to concentrate under pressure

Publications

[1]   Y. Sticker, F. Breitenecker, J. Kropf; Dynamische Simulation des
        Herzkreislaufs, Proc. ASIM 2002 Conf., Rostock, Germany.

[2]   J. Kropf; Dynamische Herzkreislaufsimulation unter Berücksich-
        tigung verteilter Parameter; Diploma Thesis, 2003.

[3]   J. Kropf, F. Breitenecker, S. Wassertheurer, M. Wibmer; Dy-
        namische Herzkreislaufsimulation unter Berücksichtigung verteil-
        ter Parameter; Proc. ASIM 2003 Conf., Magdeburg, Germany.

[4]   J. Kropf, M. Wibmer, S. Wassertheurer, J. Krocza; An Identifi-
        able Model for Dynamic Simulation of the Human Cardiovascular
        System; Proc. Eurosim 2004 Conf., Paris, France.

[5]   S. Wassertheurer, J. Kropf, F. Breitenecker, D. Magometschnigg;
        Ein generalisiertes Modell zur dynamischen Herzkreislaufsimula-
        tion; Proc. Symposium der ÖGBMT im Jahr 2004, Graz, Aus-
        tria.

[6]   D. Leitner, J. Kropf, S. Wassertheurer, F. Breitenecker; Ein Lat-
        tice Boltzmann Modell zur Simulation von lokalem Blutfluss;
        Proc. Symposium der ÖGBMT im Jahr 2005, Innsbruck, Austria.

[7]   D. Leitner, J. Kropf, S. Wassertheurer, F. Breitenecker: "Lattice
        Boltzmann Methode zur Simulation von Strömungsverhalten in
        Arterien"; Vortrag: ASIM 2005 - 18. Symposium Simulation-
        stechnik, Erlangen, Germany; 12.09.2005 - 15.09.2009; in: "Sim-
        ulation Technique - 18th Symposium Simulation Technique in
        Erlangen", F. Hülsemann, M. Kowarschik, U. Rüde (Hrg.); Fron-
        tiers in Simulation - ASIM Fortschritte in der Simulationstechnik
        / SCS Publishing House, FS 18 (2005), 3-936150-41-9; S. 768 -
        773.

[8]   J. Kropf, O. Andryushchenko: "Simulation of a Control for a
        Robot with Two Degrees of Freedom - an E-learning Example";
        Simulation News Europe SNE, 16 (2006), 1; S. 25 - 26.

[9]   J. Kropf, F. Breitenecker: "Features of Simulation Software
        for Control - Case Study for Crane Grab"; Electrical Machine-
        Building and Electrical Equipment, 2006 (2006), 66; S. 393 - 394.

[10]   F. Breitenecker, J. Kropf: "Evaluation and Comparison of Simu-
        lation Software for Mechatronic Processes - the ARGESIM Bench-
        marks"; Electrical Machine-Building and Electrical Equipment,
        2006 (2006), 66; S. 381 - 382.